AMERICAN SOCIETY FOR MICROBIOLOGY | mBio®

RESEARCH ARTICLE

Salmonella Suppresses the TRIF-Dependent Type I Interferon Response in Macrophages

Katherine A. Owen,[a] C. J. Anderson,[b] James E. Casanova[a,b]

Departments of Cell Biology[a] and Microbiology, Immunology and Cancer Biology,[b] University of Virginia Health System, Charlottesville, Virginia, USA

ABSTRACT ***Salmonella enterica* is an intracellular pathogen that causes diseases ranging from gastroenteritis to typhoid fever. *Salmonella* bacteria trigger an autophagic response in host cells upon infection but have evolved mechanisms for suppressing this response, thereby enhancing intracellular survival. We recently reported that *S. enterica* serovar Typhimurium actively recruits the host tyrosine kinase focal adhesion kinase (FAK) to the surface of the *Salmonella*-containing vacuole (SCV) (K. A. Owen et al., PLoS Pathog 10:e1004159, 2014). FAK then suppresses autophagy through activation of the Akt/mTORC1 signaling pathway. In FAK$^{-/-}$ macrophages, bacteria are captured in autophagosomes and intracellular survival is attenuated. Here we show that the cell-autonomous bacterial suppression of autophagy also suppresses the broader innate immune response by inhibiting production of beta interferon (IFN-β). Induction of bacterial autophagy (xenophagy), but not autophagy alone, triggers IFN-β production through a pathway involving the adapter TRIF and endosomal Toll-like receptor 3 (TLR3) and TLR4. Selective FAK knockout in macrophages resulted in rapid bacterial clearance from mucosal tissues after oral infection. Clearance correlated with increased IFN-β production by intestinal macrophages and with IFN-β-dependent induction of IFN-γ by intestinal NK cells. Blockade of either IFN-β or IFN-γ increased host susceptibility to infection, whereas experimental induction of IFN-β was protective. Thus, bacterial suppression of autophagy not only enhances cell-autonomous survival but also suppresses more-systemic innate immune responses by limiting type I and type II interferons.**

IMPORTANCE ***Salmonella enterica* serovar Typhimurium represents one of the most commonly identified bacterial causes of foodborne illness worldwide. *S.* Typhimurium has developed numerous strategies to evade detection by the host immune system. Autophagy is a cellular process that involves the recognition and degradation of defective proteins and organelles. More recently, autophagy has been described as an important means by which host cells recognize and eliminate invading intracellular pathogens and plays a key role in the production of cytokines. Previously, we determined that *Salmonella* bacteria are able to suppress their own autophagic capture and elimination by macrophages. Building on that study, we show here that the inhibition of autophagy by *Salmonella* also prevents the induction of a protective cytokine response mediated by beta interferon (IFN-β) and IFN-γ. Together, these findings identify a novel virulence strategy whereby *Salmonella* bacteria prevent cell autonomous elimination via autophagy and suppress the activation of innate immune responses.**

Received 20 November 2015 **Accepted** 22 January 2016 **Published** 16 February 2016

Citation Owen KA, Anderson CJ, Casanova JE. 2016. *Salmonella* suppresses the TRIF-dependent type I interferon response in macrophages. mBio 7(1):e02051-15. doi:10.1128/mBio.02051-15.

Editor B. Brett Finlay, University of British Columbia

Address correspondence to James E. Casanova, jec9e@virginia.edu.

Salmonella enterica serovar Typhimurium is a facultative intracellular pathogen that infects a variety of animal hosts. After oral infection, *S.* Typhimurium actively invades the intestinal epithelial barrier and triggers massive inflammation (1). Once across the intestinal epithelium, *Salmonella* bacteria are internalized by phagocytes, including macrophages, neutrophils, and dendritic cells (DCs) (2). Pathogenic strains of *Salmonella* express two type III secretion systems (T3SS-1 and T3SS-2) encoded by *Salmonella* pathogenicity island 1 (SPI-1) and SPI-2, which translocate distinct arrays of virulence factors into host cells. Bacterial effectors associated with T3SS-1 facilitate the entry of *Salmonella* into nonphagocytic cells, while those associated with T3SS-2 play an important role in shaping the intracellular replication niche known as the *Salmonella*-containing vacuole (SCV) (3, 4). Both sets of effectors strongly impact the induction of inflammation and the systemic spread of the pathogen, and the loss of either T3SS renders the bacteria attenuated for virulence (5–7).

Autophagy is a conserved intracellular degradation pathway that plays a critical role in the host immune response to intracellular microbes. During microbe-induced autophagy, portions of the cytoplasm that include invading bacteria or their products are sequestered in double-membrane autophagosomes before fusion with lysosomes to generate degradative autolysosomes (8–10). Importantly, autophagy has been shown to restrict the growth of a number of intracellular pathogens, including *Streptococcus pyogenes*, *Mycobacterium tuberculosis*, and *S.* Typhimurium (11–13). In the case of invasive *S.* Typhimurium, transient T3SS-1-mediated permeabilization of the SCV allows cytoplasmic components, including ubiquitin and the autophagy adapters p62, optineurin, and NDP52, to target damaged vacuoles or free bacteria

in the cytoplasm (13). Loss of essential autophagy components, such as autophagy protein 5 (Atg5), results in the unrestricted growth of *Salmonella* in fibroblasts *in vitro* (14). In addition, mice harboring intestinal epithelial cell-specific deletions of the autophagy protein Atg16L1 or Atg5 are more susceptible to *Salmonella* infection *in vivo* (15, 16).

Many intracellular pathogens have evolved strategies that antagonize autophagy initiation, evade autophagic recognition, or use components of the autophagy system to facilitate intracellular growth (17–19). Indeed, we have shown previously that the SPI-2 which encoded T3SS-2, which is upregulated upon internalization of *Salmonella* by host cells, mediates active suppression of autophagic signaling in macrophages (20). *S.* Typhimurium specifically activates the host molecule focal adhesion kinase (FAK), which is recruited to SCVs in a T3SS-2-dependent manner. FAK then triggers activation of the Akt-mTORC1 signaling axis, resulting in downregulation of the autophagic response. Importantly, FAK-deficient macrophages fail to activate Akt-mTORC1 signaling, leading to more efficient autophagic capture of *Salmonella* and reduced bacterial survival.

The induction of antimicrobial autophagy acts in conjunction with other innate immune pathways, including type I interferon (IFN) production, inflammasome signaling, and signaling of retinoic acid-inducible gene I (RIG-I)-like helicase receptors (RLRs) (21). Type I interferons (alpha interferon [IFN-α] subtypes, IFN-β, and IFN-ω) are pleiotropic cytokines that induce antiviral, antiproliferative, and immunomodulatory effects in cells. Previous studies have determined that autophagy is involved in both the positive and negative regulation of these cytokines. For example, in plasmacytoid dendritic cells (pDCs), autophagy inhibition suppresses viral recognition and the induction of type I IFNs (22, 23). In contrast, Atg5-deficient mouse embryonic fibroblasts (MEFs) were found to be resistant to viral replication, and this was attributed to the hyperproduction of type I interferons in response to immunostimulatory RNA (24). Atg9 has also recently been reported to downregulate interferon-stimulatory DNA (ISD)-mediated type I IFN production in MEFs (25). Thus, autophagy genes can positively or negatively regulate type I IFN signaling in a cell type-dependent and stimulus-dependent manner, and in some cases this involves noncanonical roles of Atg genes.

Although it is well established that the type I IFN response to viral infection is protective, its role in containing bacterial infections is less well understood and may be pathogen specific. In some cases, the IFN response is beneficial to the host (26, 27), while it has been shown in other cases to impair bacterial clearance (28). Here we show that the ability of *Salmonella* to suppress the autophagic response also results in suppression of the induction of IFN-β in macrophages. In contrast, autophagic capture of *Salmonella* enhances IFN-β production through a mechanism that requires endosomal Toll-like receptor 3 (TLR3) and TLR4 but not the cytosolic nucleotide sensor cGAS/stimulator of IFN genes (STING) or MDA-5/RIG-I. After oral infection, bacterial suppression of autophagy limits local interferon production, leading to efficient colonization and systemic dissemination. If autophagy is not suppressed (i.e., in the absence of FAK), colonization is attenuated, in a manner that is dependent on mucosal IFN-β production by macrophages and the coordinated secretion of IFN-γ by NK cells *in vivo*.

RESULTS

Autophagy enhances production of IFN-β in *Salmonella*-infected macrophages. While intracellular *Salmonella* bacteria are largely contained within the SCV in epithelia, the SPI-1 invasion machinery has been shown to perforate the SCV membrane, allowing recognition of bacteria by cytosolic pattern recognition receptors (PRRs). However, the majority of invasion-associated genes are downregulated after entry into host cells (4, 29, 30), and it is likely that *Salmonella* bacteria that have penetrated the intestinal epithelium are captured passively by mucosal macrophages. To mimic this process, *in vitro* experiments were performed with a mutant of *S.* Typhimurium strain SL1344 that lacks a functional SPI-1 T3SS (the Δ*invG* mutant).

Many intracellular pathogens induce expression of type I interferons (IFN-α/β) through recognition of bacterial pathogen-associated molecular patterns (PAMPs) by pattern recognition receptors located at the cell surface and in the cytosol (31–34; for a review, see reference 35). For example, it is well established that lipopolysaccharide (LPS) stimulation of macrophages results in the production of IFN-β (36). In accordance with this, we observed a 10-fold increase in IFN-β transcription upon treatment of wild-type (WT) mouse peritoneal macrophages (PEMs) with *Salmonella* LPS (Fig. 1A). Interestingly, however, WT macrophages incubated with noninvasive (Δ*invG*) *S.* Typhimurium for 5 h failed to upregulate IFN-β despite the presence of LPS, suggesting that *Salmonella* bacteria are capable of repressing this response (Fig. 1A).

We showed previously that *S.* Typhimurium is also able to suppress autophagy in macrophages by recruiting FAK to the cytoplasmic face of the SCV, where it stimulates the Akt/mTORC1 signaling pathway (20). If this suppressive mechanism is not operational (i.e., in the absence of FAK), macrophages mount a robust autophagic response to intracellular *Salmonella* that results in efficient bacterial clearance (see Fig. S1A in the supplemental material) (20). Since autophagy plays a major role in the biogenesis and secretion of cytokines, including type I interferons, we next examined whether enhanced autophagy could alleviate *Salmonella*-induced suppression of the type I IFN response. PEMs derived from WT or FAK$^{-/-}$ mice were incubated with noninvasive (Δ*invG*) *S.* Typhimurium for 5 h, after which IFN-β and IFN-α mRNA levels were evaluated by quantitative PCR (qPCR). As shown in Fig. 1B, infection induced a significant increase in levels of IFN-β, but not IFN-α, in FAK$^{-/-}$ PEMs compared to WT controls, with similar results observed in FAK-depleted primary immortalized macrophages (iMacs) (WT bone marrow-derived macrophages [BMDMs]) (see Fig. S1B and C). The transcriptional upregulation of IFN-β levels observed in *Salmonella*-infected FAK$^{-/-}$ PEMs correlated with a proportional increase in IFN-β protein expression (Fig. 1C and D).

The interferon response factors (IRFs) are critical regulators of the type I IFN response. While both IRF-3 and IRF-7 are activated downstream of similar signaling pathways involving TRAF3 and TRAF6, activation of IRF-3 induces transcription of IFN-β, whereas activation of IRF-7 preferentially stimulates IFN-α (37, 38). In contrast to WT PEMs, infection of FAK-deficient macrophages triggered robust activation of the IRF-3-activating kinase TBK1 and a corresponding increase in IRF-3 phosphorylation (Fig. 1E). Consistent with the absence of IFN-α induction, infection failed to activate IRF-7 in either WT or FAK$^{-/-}$ macrophages

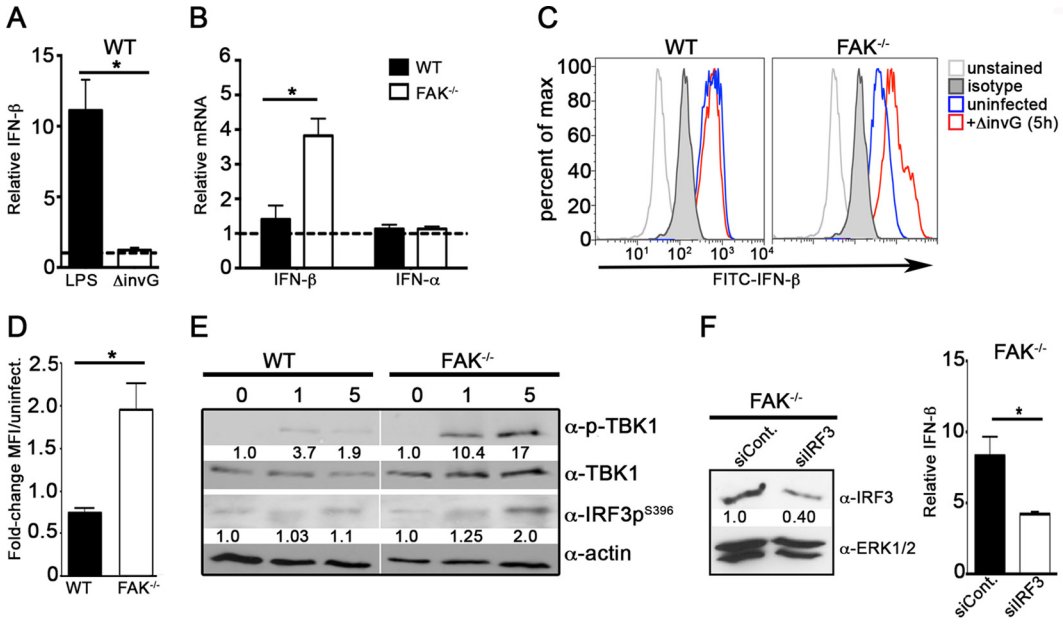

FIGURE 1 FAK deficiency in macrophages promotes IFN-β production in response to *Salmonella* infection. (A) Relative levels of expression of IFN-β mRNA by WT PEMs 5 h posttreatment with *Salmonella* LPS (100 ng/ml) or postinfection with the *S.* Typhimurium Δ*invG* strain (MOI, 100). Levels of IFN-β mRNA are displayed relative to those seen with untreated/uninfected macrophages, which were assigned a value of 1 (see hashed line). *, $P < 0.05$; $n = 5$. (B) Relative levels of expression of IFN-β and IFN-α6 mRNA by WT and FAK$^{-/-}$ PEMs 5 h postinfection with the *S.* Typhimurium Δ*invG* strain (MOI, 100). Levels of IFN-β and IFN-α6 mRNA are displayed relative to those seen with uninfected PEMs, which were assigned a value of 1 (horizontal dashed line). *, $P < 0.05$; $n = 5$. (C) WT and FAK$^{-/-}$ PEMs were incubated for 5 h with the *S.* Typhimurium Δ*invG* strain before intracellular cytokine staining for IFN-β and analysis by flow cytometry. max, maximum. (D) The mean fluorescence intensities (MFIs) of cells analyzed as described for panel C were calculated and normalized to those of uninfected controls. Data are expressed as fold change compared to uninfected cells. *, $P < 0.05$; $n = 3$. (E) WT and FAK$^{-/-}$ PEMs were incubated for 0, 1, or 5 h with the *S.* Typhimurium Δ*invG* strain before immunoblotting with the indicated antibodies. Separation of WT and FAK$^{-/-}$ immunoblots indicates noncontiguous lanes generated from a single exposure; $n = 3$. (F) FAK$^{-/-}$ PEMs were depleted of IRF-3 before immunoblotting with the indicated antibodies. Small interfering control (siCont.) and siIRF-3-treated FAK$^{-/-}$ macrophages were incubated for 5 h with the *S.* Typhimurium Δ*invG* strain, and levels of IFN-β mRNA in infected cells were calculated relative to those seen with uninfected controls. *, $P < 0.05$; $n = 3$. Statistical significance was determined using a Student's *t* test; error bars represent standard errors of the means (SEM). Densitometry was calculated using ImageJ.

(see Fig. S1D in the supplemental material). To confirm the involvement of IRF-3 in the induction of IFN-β, small interfering RNA (siRNA)-mediated depletion of IRF-3 from FAK$^{-/-}$ macrophages resulted in a significant decrease in IFN-β mRNA levels compared to control cell results during infection (Fig. 1F). Together, these results suggest that the autophagic capture of intracellular *Salmonella* increases the production of IFN-β by enhancing signaling through the TBK1/IRF3 pathway.

A weak IFN-β response in *Salmonella*-infected macrophages is amplified by autophagy. We next addressed whether the *Salmonella*-mediated induction of IFN-β expression observed in FAK$^{-/-}$ macrophages was dependent on autophagy. As shown in Fig. 2A, treatment of uninfected macrophages with the autophagy-inducing agent rapamycin (sirolimus) did not result in the activation of TBK1 or IRF-3, indicating that autophagy in the absence of bacteria is not sufficient to drive this pathway. However, the activation of both TBK1 and IRF-3 was significantly enhanced following rapamycin treatment in WT macrophages infected with *Salmonella* (Fig. 2A), and this was coincident with elevated IFN-β mRNA expression (Fig. 2B). As expected, *Salmonella* infection alone induced robust TBK-1 and IRF-3 phosphorylation in FAK$^{-/-}$ macrophages which did not increase further in the presence of rapamycin (Fig. 2A). To confirm that this response was dependent upon autophagy, FAK$^{-/-}$ macrophages were depleted of the essential autophagy component Atg5, which strongly inhibited both IRF-3 activation and IFN-β induction (Fig. 2C and D). Similarly, treatment of FAK$^{-/-}$ cells with the autophagy inhibitor 3-methyladenine (3-MA) also significantly reduced IFN-β expression (Fig. 2E). Together, these data show that pathogen stimulation is required to trigger the TBK1–IRF-3–IFN-β pathway and that this response is enhanced under autophagy-promoting conditions.

TRIF mediates IFN-β induction in FAK$^{-/-}$ macrophages following *Salmonella* infection. FAK deficiency promotes both the autophagic capture of *Salmonella* (see Fig. S1A in the supplemental material) (20) and the subsequent induction of IFN-β during infection (Fig. 1). However, it remained unclear how pathogen-mediated autophagy triggers the interferon response. We reasoned that autophagy may represent an important means through which bacterial products are delivered to intracellular pattern recognition receptors, ultimately leading to IFN-β production.

We had shown previously that nearly all (85% to 95%) internalized Δ*invG Salmonella* bacteria in macrophages are contained within undamaged SCVs, making it unlikely that recognition occurs directly in the cytosol (20). This is also consistent with the fact that we found no evidence of inflammasome activation in either WT or FAK-deficient macrophages (as determined by caspase-1 cleavage) after incubation with noninvasive *Salmonella* (see Fig. S2A in the supplemental material). Nonetheless, to test whether cytosolic nucleic acid sensors are involved in upregulating IFN-β, we examined IRF-3 activation and IFN-β levels in

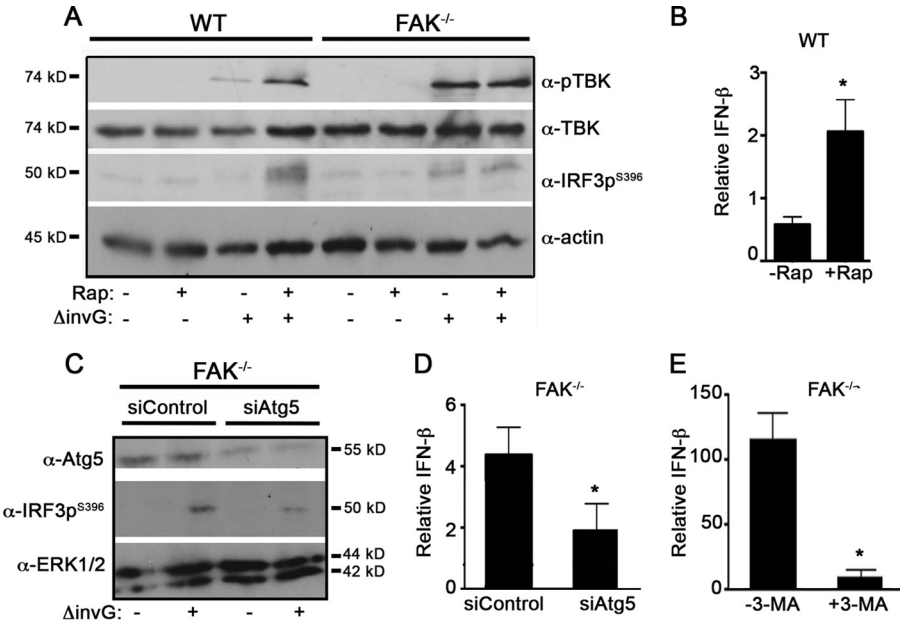

FIGURE 2 Atg5 drives IFN-β production during *Salmonella* infection. (A) WT and FAK$^{-/-}$ PEMs were pretreated with rapamycin (1 nM) for 1 h or left untreated before incubation with the *S.* Typhimurium Δ*invG* strain (MOI, 100) for 5 h. Lysates were immunoblotted with the indicated antibodies; $n = 3$. (B) WT PEMs were treated as described for panel A, and IFN-β mRNA levels in infected cells were calculated relative to those seen with uninfected controls. *, $P < 0.05$; $n = 3$. (C) FAK$^{-/-}$ PEMs were depleted of Atg5 before incubation with the *S.* Typhimurium Δ*invG* strain for 5 h. Lysates were immunoblotted with the indicated antibodies; $n = 3$. (D and E) FAK$^{-/-}$ PEMs were either depleted of Atg5 (D) or treated with the autophagy inhibitor 3-MA (5 mM) (E) before incubation for 5 h with the *S.* Typhimurium Δ*invG* strain. Levels of IFN-β mRNA in infected cells were calculated relative to those seen with uninfected controls. *, $P < 0.05$; $n = 3$. Statistical significance was determined using a Student's *t* test; error bars represent SEM.

macrophages derived from mice lacking mitochondrial antiviral signaling (MAVS) or in cells depleted of STING. MAVS is an adapter molecule that couples the double-stranded RNA (dsRNA) recognition molecules RIG-I and MDA5 to IFN-β induction (39), whereas STING functions downstream of cytoplasmic DNA sensors to induce IFN-β (40). The loss of MAVS failed to inhibit autophagy-driven IRF-3 activation or the induction of IFN-β, regardless of whether autophagy was induced by rapamycin treatment (see Fig. S2B and C) or FAK depletion (see Fig. S2D and E). Similarly, STING depletion in autophagic FAK$^{-/-}$ macrophages failed to suppress IFN-β levels upon incubation with *Salmonella* (see Fig. S2F). Importantly, neither the loss of MAVS nor depletion of STING inhibited bacterial internalization (see Fig. S2G) or the autophagic capture of bacteria (see Fig. S2H). Together, these data indicate that nucleic acids derived from Δ*invG Salmonella* are not detected by cytosolic PRRs under autophagic conditions.

Similarly to the RLRs and STING, endosomal Toll-like receptors (TLRs) recognize microbial nucleic acids but signal via the adaptor molecules MyD88 or TRIF to initiate type I IFN responses. In contrast to MAVS- and STING-deficient cells, we found that IRF-3 activation and IFN-β induction were completely abolished in cells lacking both MyD88 and TRIF, regardless of whether autophagy was induced by rapamycin treatment (Fig. 3A and C) or FAK depletion (Fig. 3B and C). Again, differences in IRF-3 signaling and IFN-β levels were not the result of altered bacterial uptake, as MyD88/TRIF knockout macrophages internalized the same number of bacteria as WT control cells (see Fig. S2G in the supplemental material).

To determine whether MyD88 or TRIF is responsible for the upregulation of IFN-β, WT macrophages depleted of either protein individually were treated with rapamycin before infection with *Salmonella*. As shown in Fig. 3D and E, depletion of TRIF but not MyD88 resulted in reduced IRF-3 activation and IFN-β induction. Similarly, FAK$^{-/-}$ macrophages depleted of TRIF (Fig. 3F and H) also failed to induce IRF-3 activation or IFN-β transcription compared to MyD88-depleted FAK$^{-/-}$ macrophages (Fig. 3G and H).

To examine whether TRIF-mediated signaling is critical for the efficient elimination of *Salmonella*, FAK$^{-/-}$ macrophages depleted of TRIF were incubated with Δ*invG Salmonella* for 3 h before bacterial survival was assessed. We found that TRIF depletion promoted bacterial survival and proliferation compared to control cell results (Fig. 3I). In contrast, stimulation of the TRIF pathway with poly(I:C), a dsRNA analog that functions as a potent TLR3 agonist and inducer of IFN-β, in WT macrophages resulted in a significant decrease in bacterial survival (Fig. 3J). Together, these data confirm that TRIF, rather than MyD88, is required for the autophagy-mediated enhancement of IFN-β production.

The IFN-β response to autophagic killing of *Salmonella* is mediated by both TLR3 and TLR4. We next examined whether the induction of IFN-β was dependent on the activity of TLR3 and/or TLR4, as these are the only intracellular TLRs that utilize TRIF for downstream signaling. To do this, TLR4-deficient macrophages were treated with rapamycin before incubation with bacteria. We found that while macrophages lacking TLR4 internalized the same number of bacteria as control macrophages (see Fig. S2G in the supplemental material), they failed to activate IRF-3 or induce IFN-β whether autophagy was induced with rapamycin or not (Fig. 4A and C). Similar results were observed in TLR4$^{-/-}$ macrophages depleted of FAK (Fig. 4B and C). Addi-

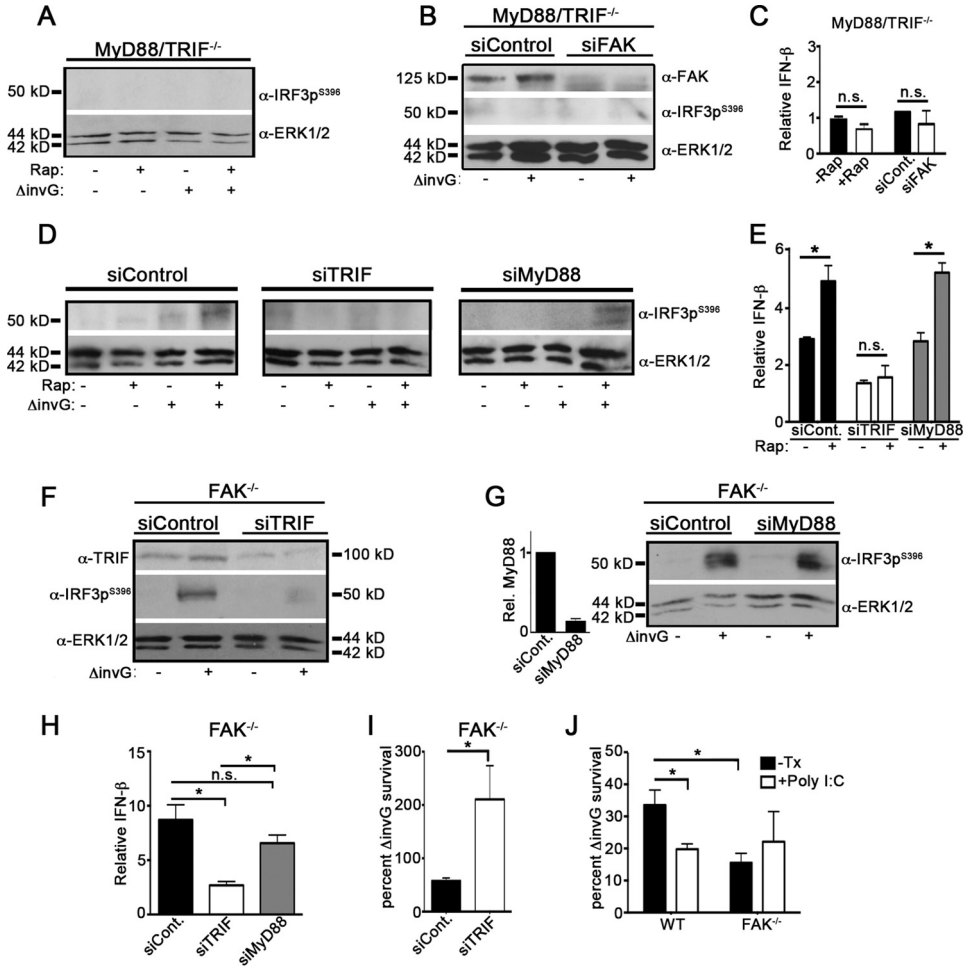

FIGURE 3 IFN-β production in response to *Salmonella* infection requires TRIF. (A and B) Immortalized macrophages (iMacs) deficient in both MyD88 and TRIF (MyD88$^{-/-}$/TRIF$^{-/-}$) were pretreated with rapamycin (1 nM) for 1 h (A) or were depleted of FAK by siRNA before incubation with Δ*invG Salmonella* (B) (MOI, 100) for 5 h. Lysates were immunoblotted with the indicated antibodies; $n = 3$. (C) Macrophages were treated as described for panels A and B before assessment of IFN-β mRNA levels. IFN-β amounts in infected cells were calculated relative to those seen with uninfected controls. n.s., not significant; $n = 3$. (D) WT iMacs were depleted of TRIF or MyD88 before pretreatment with rapamycin (1 nM) for 1 h prior to infection with Δ*InvG Salmonella* for 5 h. Lysates were immunoblotted with the indicated antibodies; $n = 3$. (E) Macrophages were treated as described for panel D before assessment of IFN-β mRNA levels. IFN-β amounts in infected cells were calculated relative to those seen with uninfected controls. *, $P < 0.05$; n.s., not significant; $n = 3$. (F and G) FAK$^{-/-}$ macrophages were depleted of TRIF or MyD88 before infection with Δ*invG Salmonella* (MOI, 100) for 5 h. Lysates were then immunoblotted with the indicated antibodies; $n = 3$. In panel G, MyD88 knockdown efficiency was determined by assessing MyD88 mRNA levels relative to those seen with siCont.-treated cells. (H) FAK$^{-/-}$ macrophages were treated as described for panel F and G before measurement of IFN-β mRNA levels. IFN-β amounts in infected cells were calculated relative to those seen with uninfected controls. *, $P < 0.05$; $n = 3$. (I) FAK$^{-/-}$ macrophages depleted of TRIF were incubated with the *S.* Typhimurium Δ*invG* strain for 3 h. Bacterial survival was assayed using a gentamicin resistance assay. (J) WT and FAK$^{-/-}$ macrophages were left untreated or treated with 5 μg/ml poly(I:C) before incubation with the Δ*invG* strain for 3 h. Bacterial survival was then assayed as described for panel I. *, $P < 0.05$; $n = 3$. Statistical significance was determined using a Student's *t* test; error bars represent SEM.

tionally, depletion of TLR3 from either rapamycin-treated WT cells (Fig. 4D and E) or FAK$^{-/-}$ macrophages (Fig. 4F and G) resulted in a significant reduction in both IRF-3 activation and IFN-β induction after *Salmonella* infection. To further confirm the role of TLR3, which requires endosomal processing for efficient ligand recognition (41), FAK$^{-/-}$ macrophages were treated with bafilomycin A1 to inhibit endosome/lysosome protease activity before incubation with *Salmonella*. As shown in Fig. 4G, treatment of cells with bafilomycin A1 strongly inhibited the induction of IFN-β. Together, these data suggest a model whereby autophagic capture of bacteria promotes bacterial degradation and the delivery of microbial products to endosomal compartments containing TLR3 and TLR4, ultimately leading to the induction of IFN-β (Fig. 4H).

FAK is required for *Salmonella*-induced suppression of the IFN response *in vivo*. Since FAK deletion in conditional FAK knockout (FAK$^{\Delta myeloid}$) animals is restricted to macrophages (see Fig. S3A to D in the supplemental material), we can use this animal model to determine if macrophage-mediated autophagy enhances the type I IFN response to *Salmonella in vivo*.

To first examine the role of FAK in the macrophage response to *Salmonella* infection, WT and FAK$^{\Delta myeloid}$ mice were orally inoculated with fully virulent *S.* Typhimurium (strain SL1344) and tissue colonization was examined. At 2 days postinfection, we did

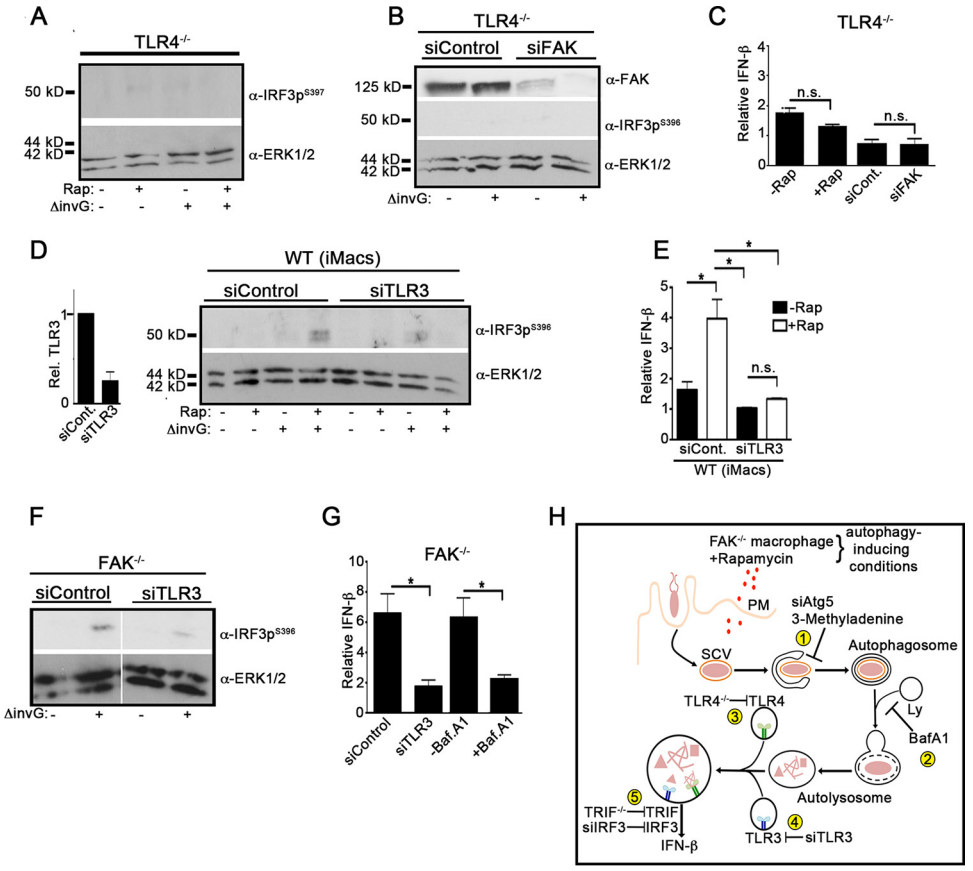

FIGURE 4 TLR3 and TLR4 are involved in IFN-β production by macrophages in response to *Salmonella* infection. (A and B) iMacs derived from TLR4-deficient mice (TLR4$^{-/-}$) were pretreated for 1 h with rapamycin (1 nM) (A) or depleted of FAK (B) before infection with Δ*invG Salmonella* (MOI, 100) for 5 h. Lysates were then immunoblotted with the indicated antibodies; $n = 3$. (C) IFN-β mRNA levels in cells treated as described for panels A and B were calculated relative to those seen with uninfected controls. n.s., not significant; $n = 3$. (D) WT iMacs depleted of TLR3 were pretreated for 1 h with rapamycin (1 nM) before infection with Δ*invG Salmonella* (MOI, 100) for 5 h. Lysates were then immunoblotted with the indicated antibodies; $n = 3$. TLR3 knockdown efficiency was determined by assessing TLR3 mRNA levels relative to those seen with siCont.-treated cells. (E) IFN-β mRNA levels in cells treated as described for panel D were calculated relative to those seen with uninfected controls. *, $P < 0.05$; $n = 3$. (F) FAK$^{-/-}$ macrophages were depleted of TLR3 before infection with Δ*invG Salmonella* (MOI, 100) for 5 h. Lysates were then immunoblotted with the indicated antibodies; $n = 3$. (G) FAK$^{-/-}$ macrophages were either treated as described for panel F or pretreated with bafilomycin A1 (Baf.A1) (100 nM) for 1 h before infection for 5 h with the *S.* Typhimurium Δ*invG* strain. IFN-β mRNA levels in infected cells were calculated relative to those seen with uninfected controls. *, $P < 0.05$; $n = 3$. Statistical significance was determined using a Student's *t* test; error bars represent SEM. (H) Model showing that autophagic conditions (FAK deletion or sirolimus treatment) promote the delivery of antigenic material to TLR-containing endosomes, resulting in IFN-β upregulation. Inhibition at each step (step 1, autophagosomes; step 2, autolysosomes; steps 3 and 4, TLR signaling; step 5, TRIF/IRF3 signaling) suppresses IFN-β. PM, plasma membrane; SCV, *Salmonella*-containing vacuole; Ly, lysosome.

not detect differences in bacterial loads recovered from the Peyer's patches (PPs) of WT and FAK$^{\Delta myeloid}$ mice (Fig. 5A); nor did we see differences between genotypes in levels of fecal bacterial shedding (see Fig. S3E in the supplemental material), indicating that bacterial invasion through the intestinal epithelium was not altered by FAK deficiency in macrophages. However, bacterial burdens were 20-fold higher in the ileum, 5-fold higher in the ceca, and 10-fold higher in the mesenteric lymph nodes (mLNs) of WT mice than in those of FAK$^{\Delta myeloid}$ littermates (Fig. 5A). This is consistent with our previous observations showing that loss of FAK from macrophages also limits the dissemination of bacteria to more distal sites such as the liver and spleen (20).

Given the upregulation in the *Salmonella*-driven IFN-β response that we observed in FAK-deficient macrophages, we next examined the ability of mice to mount a local innate immune response in the small intestine after oral infection. Using flow cytometric analysis of intracellular cytokines, we observed a significant increase in the overall proportion of IFN-β-expressing cells in the lamina propria (LP) of FAK$^{\Delta myeloid}$ mice compared to WT mice (Fig. 5B; see also Fig. S4A in the supplemental material). Among these IFN-β-producing cells, 50% to 60% were F4-80$^+$ CD11c^{lo} macrophages whereas a smaller proportion were F4-80$^+$ CD11c$^+$, a phenotype attributed to myeloid dendritic cells (DCs) (42) (Fig. 5B). We also examined IRF-3 activity in lamina propria lysates harvested from WT and FAK$^{\Delta myeloid}$ mice 2 days postinfection. Similarly to our results from infected macrophages *in vitro*, phospho-IRF-3 levels were low in WT mice but were elevated 8-fold in FAK$^{\Delta myeloid}$ mice. This is consistent with the increased number of IFN-β-producing cells in these animals (Fig. 5C).

An important consequence of IFN-β production by infected macrophages is the ability of this cytokine to stimulate the production of IFN-γ by bystander cells (43). To determine if the elevated levels of IFN-β in the LP of FAK$^{\Delta myeloid}$ mice correlated with increased IFN-γ, we next measured levels of this cytokine in

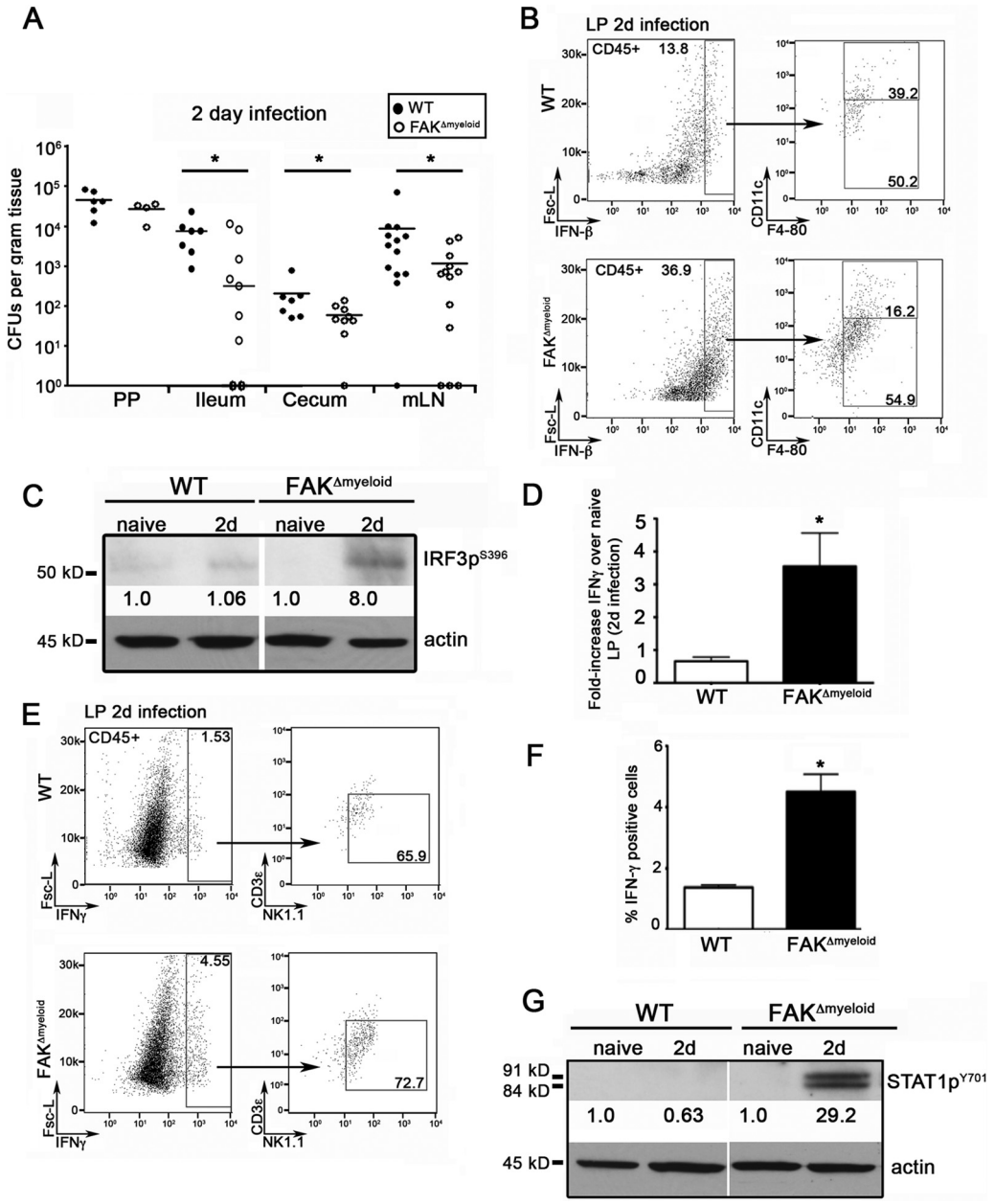

FIGURE 5 FAK deficiency improves control of *Salmonella* infection and enhances the IFN response *in vivo*. (A) Bacterial loads in WT and FAK$^{\Delta myeloid}$ mice in the indicated tissues 2 days after oral inoculation with *S.* Typhimurium strain SL1344. Each point indicates data from an individual mouse. *, $P < 0.05$ (Mann-Whitney *U* test). (B) Flow cytometric analysis of IFN-β-expressing cells in the lamina propria (LP) (taken from WT and FAK$^{\Delta myeloid}$ mice 2 days [2d] postinfection [see also Fig. S4A in the supplemental material]). The IFN-β-positive population was further analyzed for expression of CD11c and F4-80. Numbers adjacent to each gate indicate percentages of cells in the gated region. Data represent results of one of two independent experiments performed using cells pooled from three mice (6 mice total). Fsc-L, forward-scatter light. (C) Lamina propria lysates from naive and infected (2 days) WT and FAK$^{\Delta myeloid}$ mice were immunoblotted for phospho–IRF-3. Data represent results of one of three independent experiments. (D) IFN-γ levels were analyzed in LP lysates extracted from naive or infected (2 days) WT and FAK$^{\Delta myeloid}$ mice by Luminex assay. Data are expressed as fold increase in postinfection IFN-γ levels relative to those seen with naive mice. Data represent results of 3 independent experiments using LP lysates pooled from 3 mice per condition and per experiment. *, $P < 0.05$. (E) Flow cytometric analysis of IFN-γ-expressing cells in the LP (taken from WT and FAK$^{\Delta myeloid}$ mice 2 days postinfection [see also Fig. S4B]). The IFN-γ-positive population was further analyzed for expression of CD3ε and NK1.1 to identify NK cells. Numbers adjacent to each gate indicate percentages of cells in the gated region. Data are representative of results of one of three independent experiments using cells pooled from 3 mice (9 mice total). (F) Quantitation of IFN-γ-positive cells based on the flow cytometric data as described for panel B. *, $P < 0.05$. See also Table S1. (G) LP lysates from naive and infected (2 days) WT and FAK$^{\Delta myeloid}$ mice were immunoblotted with the indicated antibodies. Immunoblots represent results of one of three independent experiments. Densitometry was calculated using ImageJ. Unless indicated otherwise, statistical significance was determined using a Student's *t* test; error bars represent SEM.

WT and FAK-deficient mice 2 days after oral infection. IFN-γ levels were not significantly higher in WT mice than in control, noninfected mice (Fig. 5D). In contrast, relative IFN-γ levels in the LP increased 5-fold in FAK-deficient mice (Fig. 5D). This was correlated with a quantitatively similar increase in the levels of IFN-γ-producing cells present in the LP of FAK-deficient mice compared to WT littermates (Fig. 5E and F; see also Fig. S4B in the supplemental material).

NK cells are an important first source of IFN-γ (43). In agreement with these findings, we observed that approximately 70% of the IFN-γ-producing cells were CD3ε-negative, NK1.1-positive NK cells (Fig. 5E). This did not reflect enhanced recruitment of these cells, as the overall percentages of lamina propria NK cells remained equivalent in naive and infected animals (see Table S1 in the supplemental material). Examination of activated signal transducer and activator of transcription 1 (STAT1) levels in LP lysates revealed 30-fold induction of phospho-STAT1 in FAK-deficient mice 2 days postinfection (Fig. 5G), consistent with the elevated presence of IFN-γ in tissue lysates and a higher percentage of IFN-γ-producing cells in FAK$^{\Delta myeloid}$ animals.

IFN-β is required for the induction of IFN-γ in the small intestine and for preventing systemic dissemination of *S.* Typhimurium. To examine the importance of rapid IFN-β induction in host defense against *Salmonella* infection *in vivo*, we first blocked IFN-β signaling in mice with an antibody (Ab) against the IFN-α/β receptor IFNAR1 (Fig. 6A; see also Fig. S5A in the supplemental material) (44). Upon oral infection with WT *Salmonella* strain SL1344, mice that received the anti-IFNAR1 antibody exhibited a striking 100-fold increase in colonization of the ileum and a nearly 10-fold increase in bacterial burden in the mesenteric lymph nodes (mLNs) (Fig. 6A). Furthermore, we found that blocking IFN-β signaling partially blocked the expression of IFN-γ in the ileum of FAK-deficient mice at 48 h postinfection (Fig. 6B). To test whether the elevated level of IFN-γ observed in FAK$^{\Delta myeloid}$ animals (Fig. 5) also plays a protective role during infection, FAK-deficient animals were treated with either control IgG or neutralizing anti-IFN-γ antibodies (45) before infection with WT *S.* Typhimurium. As shown in Fig. 6A, bacterial loads in both the ileum and mLNs were significantly higher in mice treated with anti-IFN-γ antibodies than in animals receiving IgG.

Given that IFN-β is critical for protection against *Salmonella* dissemination, we next examined whether stimulation of this pathway would provide protection against infection. Control WT mice were injected intraperitoneally (i.p.) with 100 μg of IgG 1 day prior (day −1) to infection with WT *S.* Typhimurium, while animals in a second cohort were treated with 100 μg of poly(I:C) on day −1 or received poly(I:C) in addition to the anti-IFNAR1 antibody before oral infection. At 2 days postinfection, we observed a significant reduction in the bacterial burdens recovered from the small intestines of poly(I:C)-treated animals compared to control IgG-treated mice which was lost in animals receiving both poly(I:C) and anti-IFNAR1 (Fig. 6C). To further examine the protective effect of poly(I:C) treatment, WT mice were left untreated (-Tx) or administered poly(I:C) before oral inoculation with a lower, albeit lethal dose (10^8 CFU/mouse) of *S.* Typhimurium, and the clinical course of disease was followed until 10 days postinfection. Although all animals, regardless of treatment, eventually succumbed to infection, the mortality rate of poly(I:C)-treated animals was significantly lower than that of untreated control mice (7 versus 9 days) (Fig. 6D). In addition, mice receiving poly(I:C) were better able to retain weight (Fig. 6E) and exhibited significantly reduced disease activity (Fig. 6F) compared to animals receiving infection alone.

Bacterial activation of FAK suppresses the early innate immune response to *S.* Typhimurium in mLNs. CXCL9/MIG and CXCL10/IP-10 are members of the CXC class of IFN-inducible chemokines that function as potent chemoattractants for phagocytes, including neutrophils and inflammatory monocytes (46). Consistent with the upregulation in both IFN-β- and IFN-γ-expressing cells observed in *Salmonella*-infected FAK$^{\Delta myeloid}$ mice (Fig. 5), we saw a significant induction of IFN-γ, CXCL9, and CXCL10 in mLN cell lysates harvested from FAK-deficient mice relative to WT controls (Fig. 7A). Furthermore, flow cytometric analysis of myeloid populations in the mLNs showed a significantly higher percentage of activated Ly6G^{hi} neutrophils (Fig. 7B and C, region 1 [R1]; see also Fig. S4C in the supplemental material) recruited to these tissues in FAK$^{\Delta myeloid}$ animals than in control mice, whereas levels of Ly6C^{hi} inflammatory monocyte infiltration (region 2 [R2]) were equivalent between genotypes. Recently, Burton et al. (2014) determined that neutrophils were critical for limiting the spread of *Salmonella* within inflammatory lesions (47). To confirm the importance of neutrophils for *Salmonella* clearance, WT and FAK$^{\Delta myeloid}$ animals were treated with either IgG control antibodies or anti-Ly6G antibodies to deplete neutrophil levels before infection with virulent *S.* Typhimurium (see Fig. S5B). As shown in Fig. 7D, neutrophil depletion resulted in a 10-fold increase in mLN colonization of FAK-deficient mice compared to IgG-treated animals. As expected, anti-Ly6G treatment in WT animals did not impact bacterial burdens (Fig. 7D). Together, these data demonstrate that the ability of *S.* Typhimurium to manipulate FAK activity attenuates the early innate immune response to oral *Salmonella* infection and contributes to the enhanced morbidity observed in WT animals.

DISCUSSION

Type I interferons (IFNs) control a diverse array of host immune responses to infection and can be induced through both TLR-dependent and -independent mechanisms. While it is well established that type I interferons are protective in the context of antiviral immunity, the role that they play during bacterial infection is less clear and appears to depend on the bacterial species (48, 49). For example, IFN-β expression has been shown to protect against *Legionella pneumophila* (50, 51), *Chlamydia trachomatis* (52), group B streptococci, pneumococci, and *Escherichia coli* (27), whereas it exacerbates the outcome of infection with *Listeria monocytogenes* (53–55), *Francisella novicida* (56), or mycobacteria (57). In the case of *Salmonella*, the induction of type I interferon and its role in infection appear to depend on the route of entry: systemic delivery of virulent *S.* Typhimurium elicits a robust type I IFN response that actually impairs control of the pathogen (58), whereas IFN-β is barely detectable in any tissue after oral infection of WT mice (59), a finding that we confirmed in this study. Moreover, experimental induction of IFN-β through injection of the TLR3 ligand poly(I:C) was found to be protective in the context of oral *Salmonella* infection, where it enhanced bacterial clearance and reduced systemic dissemination (43). Together, these studies suggest that orally acquired *Salmonella* bacteria may in fact suppress type I IFNs in the intestinal mucosa as a novel virulence strategy.

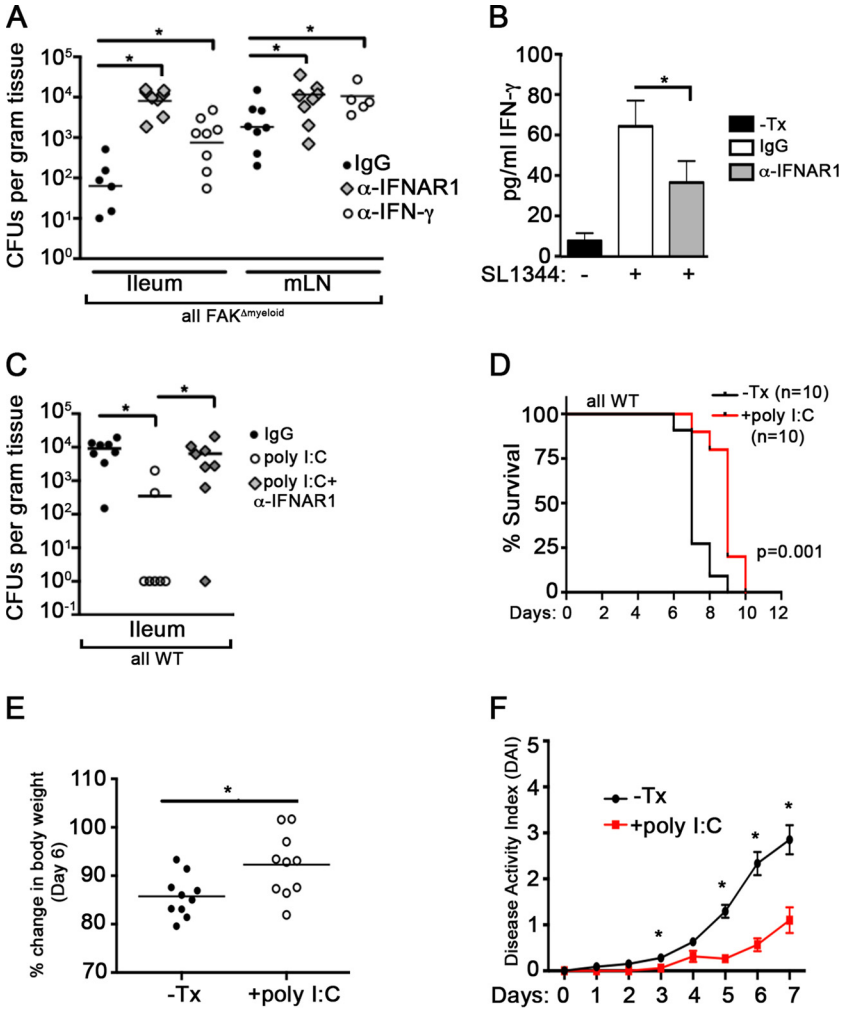

FIGURE 6 The induction of IFN-β induces protective immunity in intestinal tissues. (A) FAK$^{\Delta myeloid}$ mice were treated with control IgG, blocking anti-IFNAR1 antibodies (250 μg/mouse), or neutralizing anti-IFN-γ antibodies (250 μg/mouse) 1 day prior to infection with *S.* Typhimurium strain SL1344. Bacterial loads were assessed in the indicated tissues 2 days postinfection. Each point indicates data from an individual mouse. *, $P < 0.05$ (Mann-Whitney *U* test). (B) IFN-γ levels were analyzed in LP lysates extracted from FAK$^{\Delta myeloid}$ mice by Luminex assay. Animals were either left uninfected and untreated (-Tx) or treated with control IgG or anti-IFNAR1 antibodies (250 μg/mouse) 1 day prior to infection with SL1344 (2 days). Data represent LP lysates from 3 independent experiments. *, $P < 0.05$. (C) WT mice were treated with control IgG, poly(I:C) (100 μg/mouse), or poly(I:C) in combination with blocking anti-IFNAR1 antibodies (250 μg/mouse) 1 day prior to infection with *S.* Typhimurium strain SL1344. Bacterial loads were assessed in the ileum 2 days postinfection. Each point indicates data from an individual mouse. *, $P < 0.05$ (Mann-Whitney *U* test). (D) Kaplan-Meier survival curve for WT mice that were left untreated (-Tx) or administered poly(I:C) 1 day prior to infection with 10^8 CFU/mouse of *S.* Typhimurium strain SL1344. A total of 10 mice per condition were analyzed. (E) WT mice were treated as described for panel D. Percent change in body weight was calculated on day 6. Each point indicates data from an individual mouse. *, $P < 0.05$. (F) WT mice treated as described for panel D were assessed daily for disease activity (see Materials and Methods). Data were pooled from results of 2 independent experiments. $n = 10$; *, $P < 0.05$. Unless indicated otherwise, statistical significance was determined using a Student's *t* test; error bars represent SEM.

Autophagy is directly linked to IFN-β production in the context of bacterial infection. It is well recognized that autophagy and Atg proteins play a critical role in innate recognition of viruses and downstream cytokine responses during viral infection. Previous studies have determined that pharmacological inhibition of autophagy or Atg deficiency in plasmacytoid dendritic cells (pDCs) prevents the recognition of vesicular stomatitis virus (VSV) (22), Sendai virus (23), and human immunodeficiency virus type 1 (HIV-1) (60) through endosomal TLR7. In addition, TLR9-dependent production of type I IFN, but not proinflammatory cytokines, requires the Atg5 gene, indicating that a pathway involving Atg proteins is required for IRF7-dependent signals downstream of endosomal TLR9 (22). Thus, in the context of certain viral infections, autophagy facilitates host recognition of infection via delivery of viral ligand to the appropriate TLR-containing compartment. However, a similar mechanism for bacterial IFN induction has not yet been described.

We have previously shown that *Salmonella* contained within SCVs inhibit autophagy by activating the FAK-Akt-mTOR pathway, which prevents cell-autonomous bacterial killing (20). In the current study, we set out to determine whether this active suppression of autophagy also limits the availability of microbial degradation products capable of stimulating pattern recognition receptors and the induction of a type I interferon response. We show

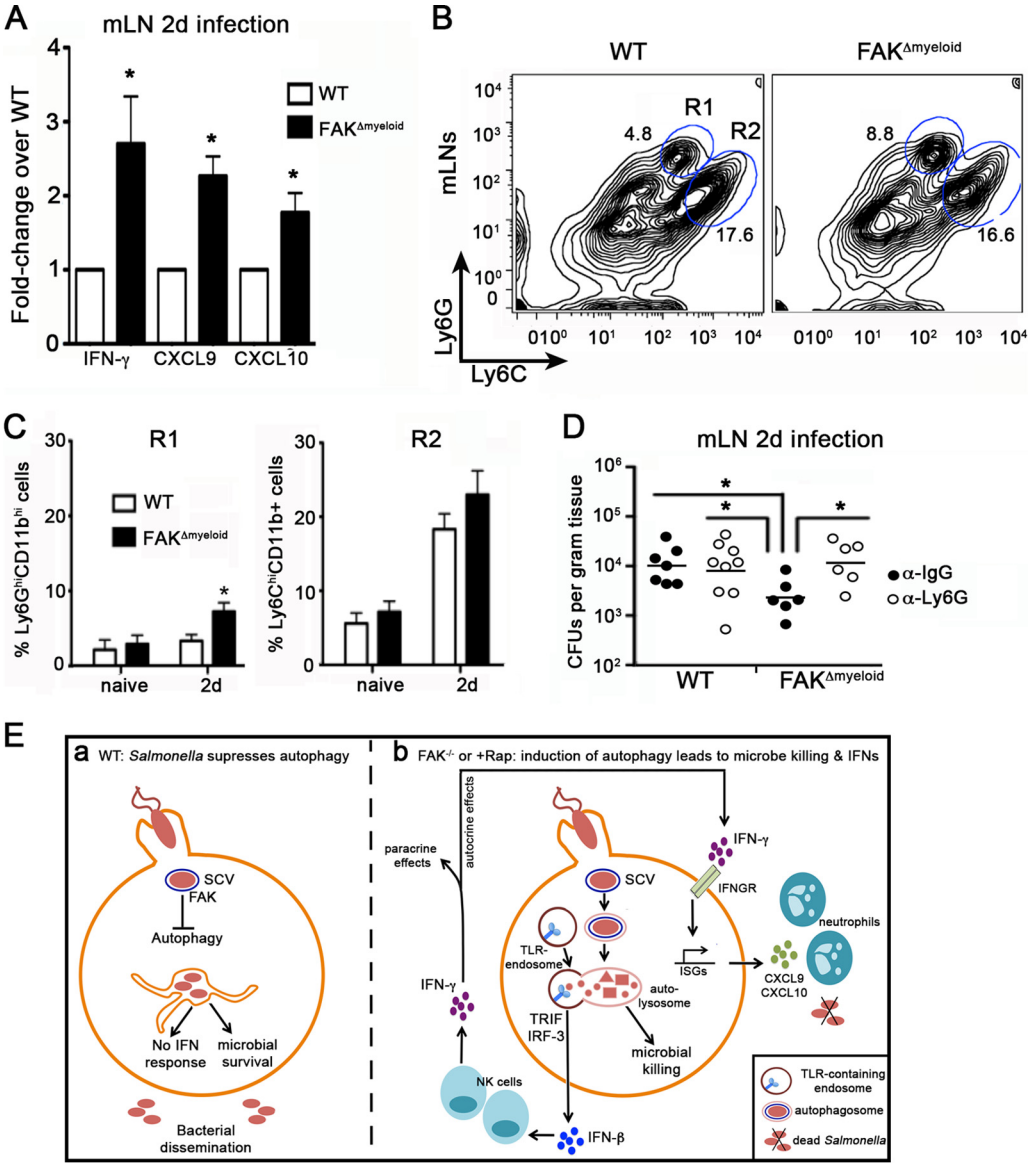

FIGURE 7 FAK$^{\Delta myeloid}$ animals exhibit an accelerated innate immune response to *Salmonella* infection. (A) mLNs from WT and FAK$^{\Delta myeloid}$ mice infected with SL1344 for 2 days were isolated and analyzed for IFN-γ, CXCL9, and CXCL10 by Luminex assay. Data are expressed as fold change relative to the WT and represent results of 3 independent experiments using mLN lysates pooled from 3 mice per experiment. *, $P < 0.05$. (B) Panels show expression of Ly6G and Ly6C in live CD45^{hi} SSC^{hi} cells from the mLNs of WT and FAK$^{\Delta myeloid}$ mice at 2 days postinfection with SL1344. Gate R1 indicates neutrophils (Ly6G^{hi} CD11b^{hi} Ly6C^{+}), and gate R2 indicates inflammatory monocytes (Ly6C^{hi} CD11b^{+}). Numbers adjacent to each gate indicate percentages of cells in R1 or R2. Data are representative of results of one of three independent experiments using cells pooled from 3 mice per experiment (see also Fig. S4C in the supplemental material). (C) Quantitation of flow cytometric data (as described for panel B) collected from naive and infected mice. *, $P < 0.05$. (D) WT and FAK$^{\Delta myeloid}$ mice were treated with control IgG or neutralizing anti-Gr1 antibodies (250 μg/mouse) 1 day prior to infection with *S.* Typhimurium strain SL1344. Bacterial loads were assessed in the mLNs 2 days postinfection. Each point indicates data from an individual mouse. *, $P < 0.05$ (Mann-Whitney *U* test). (E) Integrated working model describing the cell intrinsic and extrinsic mechanism of bacterial killing in autophagic macrophages. In WT macrophages (depicted in panel a), *Salmonella* bacteria activate the FAK-Akt-mTOR signaling pathway to suppress autophagy. Intracellular survival is enhanced, and in the absence of an IFN response, bacteria disseminate. In autophagic macrophages (panel b), *Salmonella* bacteria are captured and degraded in autophagosomes. Autophagy promotes the delivery of antigenic material to TLR-containing endosomes (see also Fig. 4H), which activates the TRIF–IRF-3 pathway to induce the production of IFN-β. IFN-β activates NK cells and promotes the production of IFN-γ. The presence of IFN-γ is able to activate additional phagocytes as well as stimulate the production of CXC chemokines. CXCL9 and CXCL10 help recruit neutrophils to the site of infection and further prevent the dissemination of bacteria.

that conditions that promote autophagy (rapamycin treatment or FAK deficiency) significantly enhance IFN-β production, while suppression of autophagy through bacterially mediated FAK-Akt-mTOR signaling, pharmacological inhibition, or knockdown of essential autophagy components impairs the IFN-β response to *Salmonella*.

Furthermore, we found that IFN-β expression in autophagic macrophages is dependent on both TLR3 and TLR4 signaling but not on MyD88, MAVS, or STING. This is consistent with the requirement for the adapter protein TRIF, which is used exclusively by endosomal TLR3 and TLR4 to activate TBK1/IRF-3. On the basis of these observations, we propose that the autophagic

degradation of *Salmonella* releases both LPS and nucleic acids into the autolysosomal lumen, where they contact TLR3 and TLR4. In support of this hypothesis, we found that neutralization of endosomal pH impaired both IRF-3 activation and IFN production. In contrast, the induction of autophagy alone by rapamycin in the absence of bacteria was not sufficient to activate TBK1 or IRF3 or stimulate IFN-β production (see model in Fig. 4).

Manipulation of IFN signaling as a virulence strategy. It should be noted that all of the *in vitro* data described above were obtained using a noninvasive strain of *S.* Typhimurium, the Δ*invG* mutant, which lacks a key component of the SPI1 T3SS. We used this strain to mimic the *in vivo* context, in which the SPI1 machinery is downregulated during transit across the intestinal epithelium (4, 29, 30).

However, we cannot rule out the possibility that some *Salmonella* bacteria are still able to actively invade macrophages in a SPI-1-dependent manner to induce type I IFN. Nonetheless, our *in vitro* and *in vivo* data suggest that by targeting FAK signaling via SPI-2, *Salmonella*-mediated suppression of the interferon response functions as an important means of survival.

To confirm that suppression of interferon production is a relevant virulence strategy *in vivo*, we infected mice orally with WT *S.* Typhimurium (SL1344). As noted above, we found that oral infection induced barely detectable IFN-β expression in WT mice, whereas it was robust in FAK$^{\Delta myeloid}$ animals. Together with our *in vitro* data, this observation suggests that by targeting FAK signaling via SPI-2, *Salmonella*-mediated suppression of the interferon response functions as an important mechanism for survival. In agreement with this hypothesis, we found that experimental induction of IFN-β with poly(I:C) (61) provides significant protection against oral *Salmonella* infection, whereas blockade of the type I interferon receptor IFNAR1 leads to increased colonization of intestinal tissues and mLNs.

The striking protective ability of IFN-β may be mediated by its immunomodulatory effect on other cell types within intestinal tissues. Previous studies have shown that IFN-β promotes the induction of IFN-γ in bystander NK cells (43, 62), which we also observed in the current study. IFN-γ is one of the most potent immunomodulatory cytokines expressed by cells, playing a critical role in antiviral, antibacterial, and antitumor responses, and functions as a bridge between innate immunity and adaptive immunity (63). Here we found that blocking IFN-γ, similarly to IFNAR1 blockade, increases bacterial burden in the ileum and mLNs, phenocopying the *Salmonella* sensitivity previously seen in interleukin-15$^{-/-}$ (IL-15$^{-/-}$) animals lacking NK cells and in IFN-$\gamma^{-/-}$ animals (64–66).

Another important aspect of the interferon response is the ability of these cytokines to activate and recruit additional leukocytes to sites of infection. In particular, CXCL9 and CXCL10 are macrophage early response genes induced in response to IFN-γ (67) that function as potent chemoattractants for T cells, NK cells, and neutrophils (68). The upregulation of both IFN-β and IFN-γ in the intestinal tissues of infected FAK$^{\Delta myeloid}$ animals correlated with increased expression of CXCL9 and CXCL10 and enhanced recruitment of neutrophils into the mLNs. It is well known that cell-mediated immunity, especially the early recruitment of neutrophils, plays a critical role in *Salmonella* clearance (47, 69). In line with this, we show that neutrophil depletion in FAK-deficient mice resulted in a significant increase in bacterial burden. Collectively, our findings suggest that enhanced survival of FAK$^{\Delta myeloid}$ animals is the result of an elevated early interferon-mediated local immune response accompanied by rapid neutrophil recruitment, which limits *Salmonella* dissemination from the intestine and mLNs.

On the basis of these observations, we propose an integrated working model whereby the autophagic capture of *Salmonella* enhances both cell-autonomous microbicidal activity (direct microbial killing in autolysosomes [20]) and more-systemic mechanisms of bacterial killing initiated by the production of IFN-β (see model in Fig. 7). In WT macrophages, activation of the *Salmonella* SPI-2 machinery specifically inhibits these responses through recruitment of FAK to the SCV. However, if autophagy is not suppressed, release of bacterial degradation products leads to activation of endosomal TLR3 and TLR4. Activation of endosomal TLRs then recruits the TRIF adapter, resulting in the activation of TBK1 and IRF-3 and the production of IFN-β. IFN-β can act in an autocrine manner to induce the expression of interferon-responsive genes in macrophages and in a paracrine manner to enhance the production of IFN-γ from local NK cells. IFN-γ not only enhances the microbicidal activity of local phagocytes but also induces expression of the potent chemoattractants CXCL9 and CXCL10. The presence of CXC chemokines recruits additional innate immune cells, such as neutrophils and monocytes, thereby preventing the dissemination of *Salmonella* bacteria that may have escaped cell-autonomous killing.

MATERIALS AND METHODS

Ethics statement. All experiments in this study were performed in strict accordance with the recommendations in the *Guide for the Care and Use of Laboratory Animals* of the National Institutes of Health. Protocols were approved by the Institutional Animal Care and Use Committee at the University of Virginia (Protocol no. 3488). All efforts were made to minimize animal suffering during the course of these studies.

Mice. The generation of myeloid-specific conditional FAK knockout mice and their control littermates has been described previously (20). Mice were kept under pathogen-free conditions and were allowed free access to food and water.

Bacterial strains and culture. *Salmonella* Typhimurium strain SL1344 and the isogenic Δ*invG* (SPI-1-deficient) invasion mutant have been described previously (20). Bacteria were grown under invasion-inducing conditions as described by Lee and Falkow (1990) (70).

Infection of mice and experimental procedures. Animals were fasted for 3 to 4 h before oral-gastric infection with 1×10^9 CFU of *Salmonella* Typhimurium strain SL1344/mouse. Mice were sacrificed 2 to 5 days postinfection, and the bacterial load in the PPs, mLN, cecum, and ileum (without PPs) was determined by plating serial dilutions of homogenized tissue suspensions on McConkey agar supplemented with 50 μg/ml of streptomycin. For some experiments, mice were administered 250 μg/mouse of monoclonal antibody (MAb) anti-IFNAR1 (MAR1-5A3), anti-Ly6G (1A8), anti-IFN-γ (XMG1.2), or IgG controls (MOPC-2 and 2A3), all purchased from BioXcell, via intraperitoneal (i.p.) injection 1 day prior to infection with SL1344. Poly(I:C) (100 μg/mouse) was also delivered by i.p. injection 1 day before infection with SL1344.

Gentamicin resistance assay. Cells were seeded at 1×10^5 to 2×10^5 cells/well onto 24-well culture dishes 18 h prior to infection. For some experiments, macrophages were treated with 5 μg/ml poly(I:C) (Sigma). Cells were then infected in complete media without antibiotics at a multiplicity of infection (MOI) of 100 for 30 min with the Δ*invG* mutant diluted in Hanks' buffered sterile saline (HBSS). Infected cells were then either lysed directly (to establish total levels of cell-associated bacteria) or treated with gentamicin (Gibco) at a concentration of 100 μg/ml for 30 min before lysis (to establish internalized bacteria), or medium was replaced with 1 μg/ml gentamycin for a further 2 h. Cells were then lysed

in 0.2% Triton X-100–HBSS. CFU were enumerated by plating aliquots of lysates onto LB agar. To determine internalized percentages, the number of CFU internalized was divided by the total number of associated CFU. To determine percent survival, the number of CFU surviving at the end of the assay (3 h) was divided by the total number of CFU internalized.

Survival analysis and DAI. To examine survival, animals were inoculated with 1×10^8 CFU SL1344/mouse (90% lethal dose [LD_{90}]) and then monitored daily for clinical symptoms of disease as defined by the disease activity index (DAI) adapted from Owen et al. (71). The DAI was calculated based on body weight, hair coat, eye discharge, activity, and posture. The total scores were determined as follows: change in weight, 0 (no change), 1 (<10% weight reduction), 2 (10% to 20%), or 3 (>20%); change in hair coat, 0 (normal, groomed), 1 (mildly rough), or 2 (very rough, ungroomed); change in eyes, 0 (normal), 1 (closed), or 2 (closed, discharge); change in activity, 0 (normal), 1 (activity with prodding), 2 (little activity with prodding), or 3 (immobile); change in posture, 0 (normal), 1 (hunched), or 2 (head on floor). Animals were sacrificed when total weight loss went below 20% or when they scored at the top of the range in 2 categories.

Flow cytometry. Single-cell suspensions were washed in fluorescence-activated cell sorter (FACS) buffer before Fc receptors were blocked by incubation with anti-CD16/32 for 15 min at 4°C. The following MAbs were purchased from BD Biosciences or eBioscience (unless otherwise stated), as conjugated to fluorescein isothiocyanate (FITC), phycoerythrin (PE), peridinin chlorophyll protein (PerCP)-Cy5.5, PE-Cy7, eFluor605NC, eFluor450, allophycocyanin (APC), or APC-Alexa Fluor 780: Ly6C (AL-21), Ly6G (IA8), Gr-1 (RB6-8C5), CD11b (M1/70), CD11c (HL3), F4-80 (BM8), CD45 (30-F11), major histocompatibility complex class II (MHC-II) (M5/114.15.2), CD62L (MEL-14), CD3ε (17A2), CD4 (L3T4), CD8 (53-6.7), NK1.1 (PK136), IFN-γ (XMG1.2), and B220 (RA3-6B2). Isotype controls included rat IgG1 conjugated to either FITC or PE. Anti-IFN-β was purchased from PBL Interferon Source. For cell sorting, single-cell suspensions were surface stained before collection using a FACSVantage SE Turbo Sorter (Becton, Dickinson). For intracellular cytokine staining, mice were i.p. injected with 500 μg monensin (Sigma-Aldrich)/mouse 6 h before tissue harvest. Intracellular IFN staining was performed using a fixation and permeabilization kit (eBioscience). IFN-positive cells were gated for surface marker analysis. Cells were collected on a CyAn ADP LX cytometer (Beckman Coulter) using Summit acquisition software (Dako) and analyzed using FlowJo software (Tree Star). For gating strategies, see Fig. S4 in the supplemental material.

Antibodies. Immunoblot analyses were performed using the following antibodies: Atg5, ERK1/2, STAT1, STAT1p^{Y701}, STING, TBK, IRF-3, phospho-TBK, and phospho-IRF3 (all purchased from Cell Signaling). Actin (cytoskeleton), caspase-1 (eBioscience), FAK (Santa Cruz Biotechnology), TRIF (Abcam), and tubulin (Sigma) antibodies were purchased from the suppliers indicated.

RNA extraction and real-time PCR. RNA extractions were performed using an RNeasy minikit (Qiagen). Expression of the IFN-β1 mRNA (interferon beta), IFN-α6 (interferon alpha), MyD88 mRNA, and TLR3 mRNA in confluent macrophage cultures infected with the Δ*invG* mutant (MOI, 100) or in untreated controls was quantified by real-time PCR. For some experiments, PEMs were pretreated with 1 nM rapamycin or 5 mM 3-MA (both purchased from Calbiochem) or with 100 nmol bafilomycin A1 (Sigma) for 1 h prior to infection. In other experiments, PEMs were treated with 100 ng/ml of *Salmonella* LPS (InvivoGen) before RNA isolation. Analysis was performed using Applied Biosystems-validated TaqMan primer-probe sets (*ifnb1*:Mm00439552_s1; *ifna6*:Mm01703458_s1; *myd88*:Mm00440338_m1; *tlr3*:Mm01207404_m1) and an ABI PRISM SDS7000 sequence detection system (Applied Biosystems). For reverse transcription, random hexamers (1 μg) and 10 ng of total RNA were used in a final reaction volume of 20 μl containing 200 units of SuperScript (Invitrogen). PCR was performed in triplicate for 40 cycles using 20% of the first-strand-synthesis volume in a total volume of 50 μl that included 25 μl of SYBR green master mix (Applied Biosystems) and a 250 nM final concentration of primers. The threshold cycle (ΔC_T) method was used to quantify all relative mRNA levels as described (ABI user guide 1997), using 18 S RNA as the reference and internal standard.

Cell culture. Peritoneal macrophages (PEMs) were isolated from mouse peritoneal lavage fluid using sterile phosphate-buffered saline (PBS) supplemented with 0.5% bovine serum albumin (BSA) and 2 mM EDTA. Bone marrow-derived macrophages (BMDMs) were isolated by flushing femurs and tibias with PBS containing 0.5% BSA and 2 mM EDTA. Both PEMs and BMDMs were seeded onto bacterial plates and cultured in alpha-minimal essential medium (alpha-MEM) supplemented with 10% heat-inactivated fetal bovine serum (FBS), 10% L929-conditioned media as a source of colony stimulating factor-1 (CSF-1), and 1% penicillin/streptomycin (pen/strep). Bone marrow-derived dendritic cells (BMDC) were generated as previously described, with slight modifications (72). Briefly, bone marrow cells removed from mouse femurs and tibias were cultured for 7 days in the presence of granulocyte-macrophage colony-stimulating factor (GM-CSF) and interleukin-4 (IL-4) (BD Biosciences), enriched for DCs by negative selection (StemCell Technologies). WT, TLR4$^{-/-}$, MAVS$^{-/-}$, and MyD88/TRIF$^{-/-}$ immortalized macrophages (iMacs) were a kind gift from Jonathan Kagan (Harvard Medical School, Boston, MA) and were cultured in primary macrophage media. J774 macrophages were cultured in Dulbecco's modified Eagle's medium (DMEM) containing 10% heat-inactivated FBS and 1% pen/strep.

Cell preparation. For LP suspensions, small intestines were excised, flushed with PBS, cut into 0.5-cm segments, and placed in shaking buffer (HBSS, 5% FBS, 2 mM EDTA) with agitation for 15 min at 37°C to remove epithelial cells. LP pieces were then digested in HBSS containing 5% FBS and 1 mg/ml collagenase IV (Sigma) with agitation for 20 min at 37°C. For mLNs, tissue was isolated and digested in collagenase IV-containing buffer as described above. Tissues were pipetted into single-cell suspensions or pressed through a nylon mesh filter (BD Falcon). Blood was obtained by cardiac puncture and immediately diluted in PBS containing 4 mM EDTA before red blood cell (RBC) lysis. For magnetic bead separation, single-cell suspensions were washed and filtered before incubation with magnetically activated cell sorting (MACS) beads (Miltenti BioTeC) conjugated to anti-CD11b, anti-CD11c, or anti-Ly6G for 15 min at 4°C. Cell suspensions were then washed and passed through a MACS column per the manufacturer's instructions before analysis by flow cytometry or lysis and immunoblotting.

Western blotting. Cells were seeded at ~1×10^5 to 2×10^5 cells/well onto 24-well culture dishes at 18 h prior to infection. For some experiments, macrophages were pretreated with rapamycin (1 nM). Cells were then rinsed twice with PBS and lysed in modified radioimmunoprecipitation assay (RIPA) buffer (50 mM Tris [pH 7.4], 1% NP-40, 150 mM NaCl, 0.5% deoxycholate, 10% glycerol, 0.1% sodium dodecyl sulfate [SDS]) supplemented with 1 mM sodium vanadate, 50-mM sodium fluoride, and a cocktail of protease inhibitors (0.1-mM phenylmethylsulfonyl fluoride and 1 μg/ml each of pepstatin, leupeptin, and antipain). Samples were loaded onto 10% SDS-polyacrylamide gels and probed using the indicated antibodies.

Microscopy. PEMs were plated on glass coverslips (Fisher) overnight before infection with the Δ*invG* mutant (MOI, 100). At 30 min after infection, the medium was changed to include gentamicin (100 μg/ml) to kill extracellular bacteria before replacement with media containing 1 μg/ml gentamycin for the remainder of the assay. Cells were fixed with 4% paraformaldehyde, followed by blocking and permeabilization in 10% normal goat serum (NGS)–0.2% saponin–PBS. Primary and secondary antibodies were diluted in blocking buffer and incubated with samples for 30 min to 1 h at room temperature (RT). After being washed, coverslips were mounted using ProLong Gold anti-fade (Invitrogen). Coverslips were examined with a 60× objective on an Olympus BX51 High Magnification microscope equipped with an Olympus DP70 digital camera. Images were acquired using ImagePro software (MediaCybernetics).

Measurement of cytokines. mLN and LP cell suspensions isolated from infected or naive mice were lysed in 0.1% Triton X-100 containing a protease inhibitor cocktail (Calbiochem) before brief homogenization at 4°C. Supernatants were collected, and levels of murine cytokines and chemokines were determined by the use of a Luminex bead system and read using a Luminex 100 IS system.

siRNA nucleofection. siRNA oligonucleotides (100 ng) targeting murine Atg5, FAK, TRIF, MyD88, IRF3, STING, and nontargeting controls (Invitrogen) were nucleofected into macrophages using an Amaxa mouse macrophage Nucleofector kit (Lonza) per the manufacturer's instructions.

Statistical analysis. Kaplan-Meier survival curves were generated for infected mice. Analyses of viable CFU recovered from the tissues of infected animals were performed using the Mann-Whitney *U* test. Student's *t* test was used for the comparison of 2 independent groups. Two-way analysis of variance (ANOVA) with Tukey's multicomponent posttest was used for comparing 2 or more independent groups. All tests were performed with Prism (GraphPad Software), and a P value of <0.05 was considered statistically significant.

SUPPLEMENTARY MATERIAL

Supplemental material for this article may be found at http://mbio.asm.org/lookup/suppl/doi:10.1128/mBio.02051-15/-/DCSupplemental.

Figure S1, TIF file, 1.7 MB.
Figure S2, TIF file, 1.2 MB.
Figure S3, TIF file, 0.5 MB.
Figure S4, TIF file, 0.5 MB.
Figure S5, TIF file, 0.3 MB.
Table S1, DOCX file, 0.01 MB.

ACKNOWLEDGMENTS

We thank the members of the University of Virginia Research Histology Core, the Flow Cytometry Core, and the Advanced Microscopy Facility for their valuable assistance. We also thank members of the J. E. Casanova laboratory (University of Virginia [UVA]) for stimulating discussions and scientific input.

This work was supported by the National Institutes of Health (RO1DK58536 to J.E.C. and 5F32DK839022 to K.A.O.). The funders had no role in study design, data collection and interpretation, or the decision to submit the work for publication.

FUNDING INFORMATION

HHS | NIH | National Institute of Diabetes and Digestive and Kidney Diseases (NIDDK) provided funding to James E Casanova under grant number RO1DK58536. HHS | NIH | National Institute of Diabetes and Digestive and Kidney Diseases (NIDDK) provided funding to Katherine A. Owen under grant number 5F32DK839022.

REFERENCES

1. **Patel S, McCormick BA.** 2014. Mucosal inflammatory response to Salmonella typhimurium infection. Front Immunol **5:**311. http://dx.doi.org/10.3389/fimmu.2014.00311.
2. **Fàbrega A, Vila J.** 2013. Salmonella enterica serovar typhimurium skills to succeed in the host: virulence and regulation. Clin Microbiol Rev **26:**308–341. http://dx.doi.org/10.1128/CMR.00066-12.
3. **Figueira R, Holden DW.** 2012. Functions of the salmonella pathogenicity island 2 (SPI-2) type III secretion system effectors. Microbiology **158:**1147–1161. http://dx.doi.org/10.1099/mic.0.058115-0.
4. **Moest TP, Méresse S.** 2013. Salmonella T3SSs: successful mission of the secret(ion) agents. Curr Opin Microbiol **16:**38–44. http://dx.doi.org/10.1016/j.mib.2012.11.006.
5. **Coburn B, Li Y, Owen D, Vallance BA, Finlay BB.** 2005. Salmonella enterica serovar typhimurium pathogenicity island 2 is necessary for complete virulence in a mouse model of infectious enterocolitis. Infect Immun **73:**3219–3227. http://dx.doi.org/10.1128/IAI.73.6.3219-3227.2005.
6. **Coombes BK, Coburn BA, Potter AA, Gomis S, Mirakhur K, Li Y, Finlay BB.** 2005. Analysis of the contribution of salmonella pathogenicity islands 1 and 2 to enteric disease progression using a novel bovine ileal loop model and a murine model of infectious enterocolitis. Infect Immun **73:**7161–7169. http://dx.doi.org/10.1128/IAI.73.11.7161-7169.2005.
7. **Hapfelmeier S, Stecher B, Barthel M, Kremer M, Müller AJ, Heikenwalder M, Stallmach T, Hensel M, Pfeffer K, Akira S, Hardt WD.** 2005. The salmonella pathogenicity island (SPI)-2 and SPI-1 type III secretion systems allow salmonella serovar typhimurium to trigger colitis via MyD88-dependent and MyD88-independent mechanisms. J Immunol **174:**1675–1685. http://dx.doi.org/10.4049/jimmunol.174.3.1675.
8. **Deretic V, Saitoh T, Akira S.** 2013. Autophagy in infection, inflammation and immunity. Nat Rev Immunol **13:**722–737. http://dx.doi.org/10.1038/nri3532.
9. **Delgado MA, Deretic V.** 2009. Toll-like receptors in control of immunological autophagy. Cell Death Differ **16:**976–983. http://dx.doi.org/10.1038/cdd.2009.40.
10. **Cemma M, Brumell JH.** 2012. Interactions of pathogenic bacteria with autophagy systems. Curr Biol **22:**R540–R545. http://dx.doi.org/10.1016/j.cub.2012.06.001.
11. **Nakagawa I, Amano A, Mizushima N, Yamamoto A, Yamaguchi H, Kamimoto T, Nara A, Funao J, Nakata M, Tsuda K, Hamada S, Yoshimori T.** 2004. Autophagy defends cells against invading group A streptococcus. Science **306:**1037–1040. http://dx.doi.org/10.1126/science.1103966.
12. **Alonso S, Pethe K, Russell DG, Purdy GE.** 2007. Lysosomal killing of mycobacterium mediated by ubiquitin-derived peptides is enhanced by autophagy. Proc Natl Acad Sci U S A **104:**6031–6036. http://dx.doi.org/10.1073/pnas.0700036104.
13. **Birmingham CL, Smith AC, Bakowski MA, Yoshimori T, Brumell JH.** 2006. Autophagy controls salmonella infection in response to damage to the salmonella-containing vacuole. J Biol Chem **281:**11374–11383. http://dx.doi.org/10.1074/jbc.M509157200.
14. **Birmingham CL, Brumell JH.** 2006. Autophagy recognizes intracellular Salmonella enterica serovar typhimurium in damaged vacuoles. Autophagy **2:**156–158. http://dx.doi.org/10.4161/auto.2825.
15. **Conway KL, Kuballa P, Song JH, Patel KK, Castoreno AB, Yilmaz OH, Jijon HB, Zhang M, Aldrich LN, Villablanca EJ, Peloquin JM, Goel G, Lee IA, Mizoguchi E, Shi HN, Bhan AK, Shaw SY, Schreiber SL, Virgin HW, Shamji AF, Stappenbeck TS, Reinecker HC, Xavier RJ.** 2013. Atg16l1 is required for autophagy in intestinal epithelial cells and protection of mice from salmonella infection. Gastroenterology **145:**1347–1357. http://dx.doi.org/10.1053/j.gastro.2013.08.035.
16. **Benjamin JL, Sumpter R, Jr, Levine B, Hooper LV.** 2013. Intestinal epithelial autophagy is essential for host defense against invasive bacteria. Cell Host Microbe **13:**723–734. http://dx.doi.org/10.1016/j.chom.2013.05.004.
17. **Choy A, Roy CR.** 2013. Autophagy and bacterial infection: an evolving arms race. Trends Microbiol **21:**451–456. http://dx.doi.org/10.1016/j.tim.2013.06.009.
18. **Sorbara MT, Girardin SE.** 2015. Emerging themes in bacterial autophagy. Curr Opin Microbiol **23:**163–170. http://dx.doi.org/10.1016/j.mib.2014.11.020.
19. **Kreibich S, Emmenlauer M, Fredlund J, Rämö P, Münz C, Dehio C, Enninga J, Hardt WD.** 2015. Autophagy proteins promote repair of endosomal membranes damaged by the salmonella type 3 secretion system 1. Cell Host Microbe **18:**527–537. http://dx.doi.org/10.1016/j.chom.2015.10.015.
20. **Owen KA, Meyer CB, Bouton AH, Casanova JE.** 2014. Activation of focal adhesion kinase by salmonella suppresses autophagy via an Akt/mTOR signaling pathway and promotes bacterial survival in macrophages. PLoS Pathog **10:**e1004159. http://dx.doi.org/10.1371/journal.ppat.1004159.
21. **Sumpter R, Jr, Levine B.** 2010. Autophagy and innate immunity: triggering, targeting and tuning. Semin Cell Dev Biol **21:**699–711. http://dx.doi.org/10.1016/j.semcdb.2010.04.003.
22. **Lee HK, Lund JM, Ramanathan B, Mizushima N, Iwasaki A.** 2007. Autophagy-dependent viral recognition by plasmacytoid dendritic cells. Science **315:**1398–1401. http://dx.doi.org/10.1126/science.1136880.
23. **Manuse MJ, Briggs CM, Parks GD.** 2010. Replication-independent activation of human plasmacytoid dendritic cells by the paramyxovirus SV5 requires TLR7 and autophagy pathways. Virology **405:**383–389. http://dx.doi.org/10.1016/j.virol.2010.06.023.
24. **Jounai N, Takeshita F, Kobiyama K, Sawano A, Miyawaki A, Xin KQ, Ishii KJ, Kawai T, Akira S, Suzuki K, Okuda K.** 2007. The Atg5 Atg12 conjugate associates with innate antiviral immune responses. Proc Natl

Acad Sci U S A **104:**14050–14055. http://dx.doi.org/10.1073/pnas.0704014104.
25. **Saitoh T, Fujita N, Hayashi T, Takahara K, Satoh T, Lee H, Matsunaga K, Kageyama S, Omori H, Noda T, Yamamoto N, Kawai T, Ishii K, Takeuchi O, Yoshimori T, Akira S.** 2009. Atg9a controls dsDNA-driven dynamic translocation of STING and the innate immune response. Proc Natl Acad Sci U S A **106:**20842–20846. http://dx.doi.org/10.1073/pnas.0911267106.
26. **Karaghiosoff M, Steinborn R, Kovarik P, Kriegshäuser G, Baccarini M, Donabauer B, Reichart U, Kolbe T, Bogdan C, Leanderson T, Levy D, Decker T, Müller M.** 2003. Central role for type I interferons and Tyk2 in lipopolysaccharide-induced endotoxin shock. Nat Immunol **4:**471–477. http://dx.doi.org/10.1038/ni910.
27. **Mancuso G, Midiri A, Biondo C, Beninati C, Zummo S, Galbo R, Tomasello F, Gambuzza M, Macrì G, Ruggeri A, Leanderson T, Teti G.** 2007. Type I IFN signaling is crucial for host resistance against different species of pathogenic bacteria. J Immunol **178:**3126–3133. http://dx.doi.org/10.4049/jimmunol.178.5.3126.
28. **Manca C, Tsenova L, Bergtold A, Freeman S, Tovey M, Musser JM, Barry CE, III, Freedman VH, Kaplan G.** 2001. Virulence of a Mycobacterium tuberculosis clinical isolate in mice is determined by failure to induce Th1 type immunity and is associated with induction of IFN-alpha /beta. Proc Natl Acad Sci U S A **98:**5752–5757. http://dx.doi.org/10.1073/pnas.091096998.
29. **Drecktrah D, Knodler LA, Ireland R, Steele-Mortimer O.** 2006. The mechanism of salmonella entry determines the vacuolar environment and intracellular gene expression. Traffic **7:**39–51. http://dx.doi.org/10.1111/j.1600-0854.2005.00360.x.
30. **Ibarra JA, Knodler LA, Sturdevant DE, Virtaneva K, Carmody AB, Fischer ER, Porcella SF, Steele-Mortimer O.** 2010. Induction of salmonella pathogenicity island 1 under different growth conditions can affect salmonella-host cell interactions in vitro. Microbiology **156:**1120–1133. http://dx.doi.org/10.1099/mic.0.032896-0.
31. **De Almeida LA, Carvalho NB, Oliveira FS, Lacerda TL, Vasconcelos AC, Nogueira L, Bafica A, Silva AM, Oliveira SC.** 2011. MyD88 and STING signaling pathways are required for IRF3-mediated IFN-beta induction in response to Brucella abortus infection. PLoS One **6:**e23135. http://dx.doi.org/10.1371/journal.pone.0023135.
32. **O'Riordan M, Yi CH, Gonzales R, Lee KD, Portnoy DA.** 2002. Innate recognition of bacteria by a macrophage cytosolic surveillance pathway. Proc Natl Acad Sci U S A **99:**13861–13866. http://dx.doi.org/10.1073/pnas.202476699.
33. **Prantner D, Darville T, Nagarajan UM.** 2010. Stimulator of IFN gene is critical for induction of IFN-beta during Chlamydia muridarum infection. J Immunol **184:**2551–2560. http://dx.doi.org/10.4049/jimmunol.0903704.
34. **Gratz N, Hartweger H, Matt U, Kratochvill F, Janos M, Sigel S, Drobits B, Li XD, Knapp S, Kovarik P.** 2011. Type I interferon production induced by Streptococcus pyogenes-derived nucleic acids is required for host protection. PLoS Pathog **7:**e1001345. http://dx.doi.org/10.1371/journal.ppat.1001345.
35. **Trinchieri G.** 2010. Type I interferon: friend or foe? J Exp Med **207:**2053–2063. http://dx.doi.org/10.1084/jem.20101664.
36. **Gessani S, Belardelli F, Pecorelli A, Puddu P, Baglioni C.** 1989. Bacterial lipopolysaccharide and gamma interferon induce transcription of beta interferon mRNA and interferon secretion in murine macrophages. J Virol **63:**2785–2789.
37. **Schafer SL, Lin R, Moore PA, Hiscott J, Pitha PM.** 1998. Regulation of type I interferon gene expression by interferon regulatory factor-3. J Biol Chem **273:**2714–2720. http://dx.doi.org/10.1074/jbc.273.5.2714.
38. **Honda K, Yanai H, Negishi H, Asagiri M, Sato M, Mizutani T, Shimada N, Ohba Y, Takaoka A, Yoshida N, Taniguchi T.** 2005. IRF-7 is the master regulator of type-I interferon-dependent immune responses. Nature **434:**772–777. http://dx.doi.org/10.1038/nature03464.
39. **Reikine S, Nguyen JB, Modis Y.** 2014. Pattern recognition and signaling mechanisms of RIG-I and MDA5. Front Immunol **5:**342. http://dx.doi.org/10.3389/fimmu.2014.00342.
40. **Ishikawa H, Barber GN.** 2008. STING is an endoplasmic reticulum adaptor that facilitates innate immune signalling. Nature **455:**674–678. http://dx.doi.org/10.1038/nature07317.
41. **Qi R, Singh D, Kao CC.** 2012. Proteolytic processing regulates Toll-like receptor 3 stability and endosomal localization. J Biol Chem **287:**32617–32629. http://dx.doi.org/10.1074/jbc.M112.387803.
42. **Denning TL, Wang YC, Patel SR, Williams IR, Pulendran B.** 2007. Lamina propria macrophages and dendritic cells differentially induce regulatory and interleukin 17-producing T cell responses. Nat Immunol **8:**1086–1094. http://dx.doi.org/10.1038/ni1511.
43. **Sotolongo J, España C, Echeverry A, Siefker D, Altman N, Zaias J, Santaolalla R, Ruiz J, Schesser K, Adkins B, Fukata M.** 2011. Host innate recognition of an intestinal bacterial pathogen induces TRIF-dependent protective immunity. J Exp Med **208:**2705–2716. http://dx.doi.org/10.1084/jem.20110547.
44. **Sheehan KC, Lai KS, Dunn GP, Bruce AT, Diamond MS, Heutel JD, Dungo-Arthur C, Carrero JA, White JM, Hertzog PJ, Schreiber RD.** 2006. Blocking monoclonal antibodies specific for mouse IFN-alpha/beta receptor subunit 1 (IFNAR-1) from mice immunized by in vivo hydrodynamic transfection. J Interferon Cytokine Res **26:**804–819. http://dx.doi.org/10.1089/jir.2006.26.804.
45. **Cherwinski HM, Schumacher JH, Brown KD, Mosmann TR.** 1987. Two types of mouse helper T cell clone. III. Further differences in lymphokine synthesis between Th1 and Th2 clones revealed by RNA hybridization, functionally monospecific bioassays, and monoclonal antibodies. J Exp Med **166:**1229–1244. http://dx.doi.org/10.1084/jem.166.5.1229.
46. **Van Raemdonck K, Van den Steen PE, Liekens S, Van Damme J, Struyf S.** 2015. CXCR3 ligands in disease and therapy. Cytokine Growth Factor Rev **26:**311–327 http://dx.doi.org/10.1016/j.cytogfr.2014.11.009.
47. **Burton NA, Schürmann N, Casse O, Steeb AK, Claudi B, Zankl J, Schmidt A, Bumann D.** 2014. Disparate impact of oxidative host defenses determines the fate of salmonella during systemic infection in mice. Cell Host Microbe **15:**72–83. http://dx.doi.org/10.1016/j.chom.2013.12.006.
48. **Stetson DB, Medzhitov R.** 2006. Type I interferons in host defense. Immunity **25:**373–381. http://dx.doi.org/10.1016/j.immuni.2006.08.007.
49. **Eshleman EM, Lenz LL.** 2014. Type I interferons in bacterial infections: taming of myeloid cells and possible implications for autoimmunity. Front Immunol **5:**431. http://dx.doi.org/10.3389/fimmu.2014.00431.
50. **Plumlee CR, Lee C, Beg AA, Decker T, Shuman HA, Schindler C.** 2009. Interferons direct an effective innate response to Legionella pneumophila infection. J Biol Chem **284:**30058–30066. http://dx.doi.org/10.1074/jbc.M109.018283.
51. **Schiavoni G, Mauri C, Carlei D, Belardelli F, Pastoris MC, Proietti E.** 2004. Type I IFN protects permissive macrophages from Legionella pneumophila infection through an IFN-gamma-independent pathway. J Immunol **173:**1266–1275. http://dx.doi.org/10.4049/jimmunol.173.2.1266.
52. **Vignola MJ, Kashatus DF, Taylor GA, Counter CM, Valdivia RH.** 2010. cPLA2 regulates the expression of type I interferons and intracellular immunity to Chlamydia trachomatis. J Biol Chem **285:**21625–21635. http://dx.doi.org/10.1074/jbc.M110.103010.
53. **Auerbuch V, Brockstedt DG, Meyer-Morse N, O'Riordan M, Portnoy DA.** 2004. Mice lacking the type I interferon receptor are resistant to Listeria monocytogenes. J Exp Med **200:**527–533. http://dx.doi.org/10.1084/jem.20040976.
54. **O'Connell RM, Saha SK, Vaidya SA, Bruhn KW, Miranda GA, Zarnegar B, Perry AK, Nguyen BO, Lane TF, Taniguchi T, Miller JF, Cheng G.** 2004. Type I interferon production enhances susceptibility to Listeria monocytogenes infection. J Exp Med **200:**437–445. http://dx.doi.org/10.1084/jem.20040712.
55. **Carrero JA, Calderon B, Unanue ER.** 2004. Type I interferon sensitizes lymphocytes to apoptosis and reduces resistance to Listeria infection. J Exp Med **200:**535–540. http://dx.doi.org/10.1084/jem.20040769.
56. **Henry T, Kirimanjeswara GS, Ruby T, Jones JW, Peng K, Perret M, Ho L, Sauer JD, Iwakura Y, Metzger DW, Monack DM.** 2010. Type I IFN signaling constrains IL-17A/F secretion by gammadelta T cells during bacterial infections. J Immunol **184:**3755–3767. http://dx.doi.org/10.4049/jimmunol.0902065.
57. **Mayer-Barber KD, Andrade BB, Barber DL, Hieny S, Feng CG, Caspar P, Oland S, Gordon S, Sher A.** 2011. Innate and adaptive interferons suppress IL-1alpha and IL-1beta production by distinct pulmonary myeloid subsets during Mycobacterium tuberculosis infection. Immunity **35:**1023–1034. http://dx.doi.org/10.1016/j.immuni.2011.12.002.
58. **Robinson N, McComb S, Mulligan R, Dudani R, Krishnan L, Sad S.** 2012. Type I interferon induces necroptosis in macrophages during infection with Salmonella enterica serovar typhimurium. Nat Immunol **13:**954–962. http://dx.doi.org/10.1038/ni.2397.
59. **Tam MA, Sundquist M, Wick MJ.** 2008. MyD88 and IFN-alphabeta differentially control maturation of bystander but not salmonella-associated dendritic cells or CD11cintCD11b$^+$ cells during infection. Cell

Microbiol **10:**1517–1529. http://dx.doi.org/10.1111/j.1462-5822.2008.01144.x.

60. **Zhou D, Kang KH, Spector SA.** 2012. Production of interferon alpha by human immunodeficiency virus type 1 in human plasmacytoid dendritic cells is dependent on induction of autophagy. J Infect Dis **205:**1258–1267. http://dx.doi.org/10.1093/infdis/jis187.
61. **Tian X, Xu F, Lung WY, Meyerson C, Ghaffari AA, Cheng G, Deng JC.** 2012. Poly I:C enhances susceptibility to secondary pulmonary infections by gram-positive bacteria. PLoS One **7:**e41879. http://dx.doi.org/10.1371/journal.pone.0041879.
62. **Zhou Z, Zhang C, Zhang J, Tian Z.** 2012. Macrophages help NK cells to attack tumor cells by stimulatory NKG2D ligand but protect themselves from NK killing by inhibitory ligand Qa-1. PLoS One **7:**e36928. http://dx.doi.org/10.1371/journal.pone.0036928.
63. **Lin FC, Young HA.** 2014. Interferons: success in anti-viral immunotherapy. Cytokine Growth Factor Rev **25:**369–376. http://dx.doi.org/10.1016/j.cytogfr.2014.07.015.
64. **Bao S, Beagley KW, France MP, Shen J, Husband AJ.** 2000. Interferon-gamma plays a critical role in intestinal immunity against Salmonella typhimurium infection. Immunology **99:**464–472. http://dx.doi.org/10.1046/j.1365-2567.2000.00955.x.
65. **Ashkar AA, Reid S, Verdu EF, Zhang K, Coombes BK.** 2009. Interleukin-15 and NK1.1+ cells provide innate protection against acute Salmonella enterica serovar Typhimurium infection in the gut and in systemic tissues. Infect Immun **77:**214–222. http://dx.doi.org/10.1128/IAI.01066-08.
66. **Kupz A, Scott TA, Belz GT, Andrews DM, Greyer M, Lew AM, Brooks AG, Smyth MJ, Curtiss R, III, Bedoui S, Strugnell RA.** 2013. Contribution of Thy1+ NK cells to protective IFN-gamma production during Salmonella typhimurium infections. Proc Natl Acad Sci U S A **110:**2252–2257. http://dx.doi.org/10.1073/pnas.1222047110.
67. **Rauch I, Müller M, Decker T.** 2013. The regulation of inflammation by interferons and their STATs. JAKSTAT **2:**e23820. http://dx.doi.org/10.4161/jkst.23820.
68. **Liu M, Guo S, Hibbert JM, Jain V, Singh N, Wilson NO, Stiles JK.** 2011. CXCL10/IP-10 in infectious diseases pathogenesis and potential therapeutic implications. Cytokine Growth Factor Rev **22:**121–130. http://dx.doi.org/10.1016/j.cytogfr.2011.06.001.
69. **Rydström A, Wick MJ.** 2007. Monocyte recruitment, activation, and function in the gut-associated lymphoid tissue during oral salmonella infection. J Immunol **178:**5789–5801. http://dx.doi.org/10.4049/jimmunol.178.9.5789.
70. **Lee CA, Falkow S.** 1990. The ability of salmonella to enter mammalian cells is affected by bacterial growth state. Proc Natl Acad Sci U S A **87:**4304–4308. http://dx.doi.org/10.1073/pnas.87.11.4304.
71. **Owen KA, Abshire MY, Tilghman RW, Casanova JE, Bouton AH.** 2011. FAK regulates intestinal epithelial cell survival and proliferation during mucosal wound healing. PLoS One **6:**e23123. http://dx.doi.org/10.1371/journal.pone.0023123.
72. **Bullock TN, Colella TA, Engelhard VH.** 2000. The density of peptides displayed by dendritic cells affects immune responses to human tyrosinase and gp100 in HLA-A2 transgenic mice. J Immunol **164:**2354–2361. http://dx.doi.org/10.4049/jimmunol.164.5.2354.